Evaluation of Material Surface Profiling Methods: Contact *versus* Non-contact

A thesis submitted in partial fulfilment of the
requirements of Brunel University London
for the degree of Master of Philosophy

by

Supaporn Jaturunruangsri

College of Engineering, Design and Physical Sciences,
Brunel University London
December 2014

Abstract

Accurate determination of surface texture is essential for the manufacturing of mechanical components within design specifications in engineering and materials science disciplines. It is also required for any subsequent modifications to physical properties and functional aspects of the object. A number of methods are available to characterize any surface through the measurement of roughness parameters that can then be used to describe surface texture. These methods may be divided into those in that direct contact is made with the surface and those where such contact is not required.

This report describes two methods approach for the surface profiling of a quartz glass substrate for step height, and tungsten substrate for roughness measure. A stylus profilometer (contact method) and vertical scanning interferometer, (VSI) or (non-contact optical method) were used for step height and roughness parameter measurements. A comparison was made with nominal values assigned to the studied surface, and conclusions drawn about the relative merits of the two methods.

Those merits were found to differ, depending on the parameters under consideration. The stylus method gave better agreement of step height values for dimensions greater than a micron. Both methods showed excellent accuracy at smaller dimensions. Both methods also provided accurate average roughness values, although the VSI data significantly overestimated 35% above the peak-to-valley parameter. Likely sources and nature of such differences are discussed based on the results presented, as well as on the previous comparison studies reported in the literature.

Because of such method-specific differences, the multi-technique approach used in this work for accurate surface profiling appears to be a more rational option than reliance upon a single method. Both contact and non-contact approaches have problems with specific roughness parameters, but a hybrid approach offers the possibility of combining the strengths of both methods and eliminating their individual weaknesses.

Acknowledgement

First and foremost, I would like to express my gratitude to my supervisor, Dr Qingping Yang and Professor Kai Cheng for his valuable recommendations, guidance, motivations, encourages and support throughout this research process.

I am grateful to the Department of Science Service in Thailand for my sponsorship support to my PhD study. The thanks are also extended to Brunel University for all the support for my PhD study.

I am grateful to the Department of Dimensional Metrology, National Institute of Metrology (Thailand) and National Physical Laboratory for allowance to use instrument for my study.

The special thanks are due to my colleagues, Mr. Anusorn Tonmueanwai, Dr. Jariya Buajarern, Mr. Thammarat Somthong, Dr. JIttakant Intiang for their valuable discussions in many regards on my research work and always helpful assistance and support.

Finally, I am also thankful to my family who encourage and always standby me throughout this research study.

Table of Contents

List of Figures

List of Tables

Chapter 1

1. Introduction

1.1 The importance of surfaces

Any solid material is composed of two main parts – the bulk and the surface. The surface layer acts as an interface between the bulk of the material and its ambient environment. Consequently the surface plays a pivotal role in the chemical reactivity of the material and also in its physical interactions in the form of fundamental processes, such as friction, wear and corrosion that a material can be subjected to in an engineering environment. *Surface engineering* is the study and application of analytical and manufacturing techniques to characterize and manipulate the surfaces. The objective is to alter chemical or physical features of surfaces to produce more robust and functional materials, as well as materials that are more efficient and have a longer operational life (Davis, 2001; Batchelor et al., 2011; Takadoum, 2008).

A surface is defined by Webster's dictionary as "the two-dimensional boundary of a material body". Surface science has been important sub-fields of materials science for several decades. Surface science is inter-disciplinary, with significant contributions from physics, chemistry, biology and engineering (Whitehouse, 1994; 2011). The objectives of surface science are greater understanding of surface corrosion (Dubois and Belin-Ferré, 2011), heterogeneous catalysis processes, electrochemistry, material-tissue interfaces in medical contexts (Zhou and Breyen, 2010), solid state chemical reaction mechanics (Todres, 2006) and chemical adsorption processes. Detailed understanding of these processes and phenomena would lead to improved efficiency, cost savings in the manufacturing processes and to a reduction in the quantity of undesired products. Because surfaces are ubiquitous in all areas of science and technology, improving the efficiency of surface creation and manipulation carries considerable financial benefits to the industry.

Surface metrology is a science of measuring surfaces that is critical in many industrial processes. From an engineering point of view, surface metrology deals with the measurement

of the deviation of an object surface from its intended shape (Whitehouse, 1997; 2000, 2011). Metrology is particularly important for "structured" surfaces that carry particular patterns (a recent example being the use of patterned media for magnetic information recording). Structured surfaces are a major emerging area of engineering and any improvements in surface metrology do therefore propagate down the utilization chain to eventually benefit the human society as a whole – the global market for structured surfaces is estimated at several hundred billion dollars (Jiang and Whitehouse, 2012). It is therefore essential that the tools for the study of those surfaces are developed to a point of being reliable and easy to use, even for the challenging dimension specifications with are in nanometer scale.

Surface topography is an important characteristic that determines, among other things, catalytic activity, electrochemical potential, adhesion, friction coefficient, susceptibility to wear and scuffing failure and aesthetic appearance (Lonardo et al., 2002, Mathia et al., 2011, Whitehouse, 2011). The topography is the outcome of the surface metrology experiment. Modern technologies place very stringent requirements on the surface quality – polished surfaces have greater mechanical strength and corrosion resistance, optical surfaces often need to be polished to maintain a specific curvature down to the Angstrom level and catalysis / absorption systems must, on the contrary, have surfaces that are as rough as the physical and chemical nature of the material can possibly allow.

Surfaces are also important in chemical industry due to the multitude of physical (absorption, adsorption) and chemical (catalysis, electrochemistry, corrosion) processes that can occur on them. Roughness in particular (and surface area in general) is a very important characteristic of chemical sorbents – the amount of substance that a surface can adsorb is usually proportional to its total area (Atkins and De Paula, 2010). This area can vary very broadly – from a few square millimeters per gram (glass beads) to a few hundred square meters per gram (activated charcoal, zeolites). Catalytic processes, particularly those involving metals, are often limited to particular kinds of surfaces Given the importance of chemical catalysis to the industry (hydrogenation, carbohydrate cracking, pharmacology, nitrogen fertilizers, plastic industry, *etc.*), the demand for standard surface characterization processes is very strong – all the various catalysts (platinum, palladium, iron oxides, charcoal, nickel, *etc.*) must present specific surface

characteristic to the reaction system in order for the process to be reproducible and therefore amenable to optimization (Atkins and De Paula, 2010).

Another major area of industrial importance that essentially involves surfaces is industrial corrosion research – many types of steel or other alloys operate in aggressive chemical environments (*e.g.* salty oxygen-rich or sulphur-rich environment that surrounds steel pipes used in oil well drilling). The rate of electrochemical corrosion is a function of the surface area (Jüttner, 1990) – polished surfaces are less amenable to electrochemical corrosion processes than roughly finished ones. This is particularly true for corrosion-resistant alloys which rely on the formation of passive film of metal oxide or sulphide that prevents further corrosion processes. Smoothly finished surfaces form such films readily, whereas roughly finished ones are less likely to form a stable film and are therefore more amenable to corrosion (Tan, 2013). A reliable and reproducible surface finish characterization technique would be very useful in this context because it would allow one to predict the corrosion resistance properties of a given metallic part.

The traditional way of measuring surface topography is mechanical – all current roughness standards are defined using stylus instruments that normally use a diamond stylus. Not all surfaces can be studied in that way, however. Diamond usually scratches the surface and may be outright inapplicable to the cases where surfaces are very soft, for example in biological systems or polymer science. For this reason, the last few decades have seen the development of alternative methods that do not use a stylus. Those can be loosely divided into optical methods (such as vertical scanning interferometry) and non-optical methods (such as scanning tunneling microscopy). A very important question is about the accuracy of these methods and about the extent to which they may be superior or inferior to the stylus-based surface metrology. This thesis makes a step in that general direction and compares two popular surface profilometry methods using a set of standard samples – the outcome are a set of recommendations on the appropriateness and accuracy of each method, depending on the sample and the parameter being measured.

1.2 Physical nature of manufactured surfaces

The machining (*e.g.* cutting or cleaving) of any piece of raw material for the production of a desired object inevitably imparts on the surface of the object a number of features and patterns that deviate from an idealized or totally flat and smooth surface. Indeed in many manufacturing processes, such surface deviations are desired in order to meet design specifications and control an object's key functional properties (Evans and Bryan, 1999; Whitehouse, 2000). Some surfaces are intended to be perfectly smooth (although not necessarily flat) – a good example is optical surfaces used in aerospace applications that have to have a specific surface curvature with nanometer-scale precision. Other surfaces must intentionally be as rough as possible because their application area is catalysis or absorption (platinum black, activated charcoal and zeolites are good examples). Engineering surfaces are often required to have microscopic grooves (ball bearings operate better because traces of lubricants are collected in the grooves) and to avoid spikes (which are friction-prone and not well-lubricated). Patterned surfaces must have specific arrangements of geometric features on them, often combining several different materials.

1.2.1 Surface diagnostic parameters

The three primary diagnostic parameters that are used to describe and quantify any such surface – *lay*, *roughness* and *waviness* – are illustrated schematically in Figure 1.1.

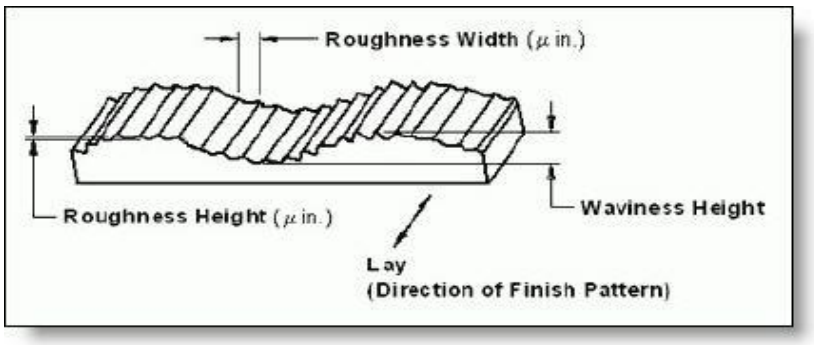

Figure 1.1 Schematic illustration of the concepts of lay, roughness and waviness that considered together describe *surface texture* (image reproduced from the Pro CNC Corporation web site, http://procnc.com).

Lay refers to the principal 'macro' pattern that the particular machining method used would produce on the surface of the final object. Roughness describes the finer 'micro' surface

irregularities present (equivalent to *surface finish* in the engineering jargon), whilst waviness is an indicator of those irregularities that reside on a spatial scale of higher order than roughness – for example the features that result from processes such as warping or vibration during the material machining stage. These three characteristics, along with their defined associated height and width parameters (described in more detail below), account for what is normally termed a material object's *surface texture* (Smith, 2002). The requirements of a particular manufactured object will dictate the precise degree to that a surface is perfected in order to reduce specific surface irregularities (Thwaite, 1984). Strict standards and definitions are set out to that end by national and international organizations, such as ISO (ISO4287, 1997; ISO4288, 1996; ISO5436, 2000; ISO25178, 2012) and ANSI (ASME-B46.1, 2009). These standards exist to ensure accuracy in terminology and unify quality standards across engineering disciplines.

1.2.2 Surface texture types

All surfaces can be classified into general categories that reflect the density and distribution of the roughness features that generate the overall surface profile (Figure 1.2). Homogeneity is the property of uniform distribution of surface features; isotropy is the property of uniformity in any and all directions and a Gaussian surface is one characterized by a particular distribution form (the Gaussian or normal) of textural features. Roughness at both micrometer (10^{-6} m) and nanometer (10^{-9} m) dimensions are a result of short spatial scale fluctuations such as localized maxima (peaks) and minima (valleys) characterized by different (amplitudes) and spacing.

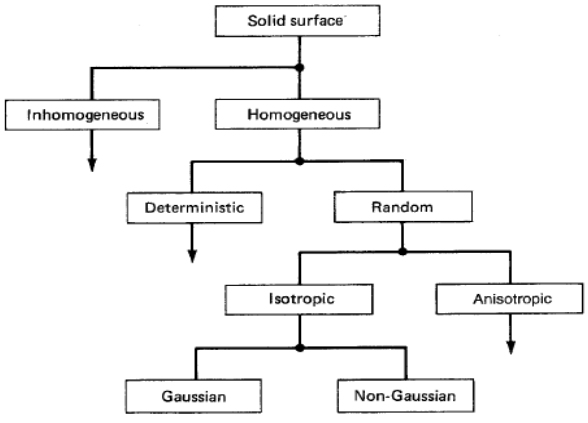

Figure 1.2 Surface texture types, reproduced from (Bhushan, 2001).

Such features are a natural consequence of any particular form of manufacturing process – there are many different forms that have characteristic roughness values associated with them (Figure 1.3). The roughness parameter R_a is defined in the following section.

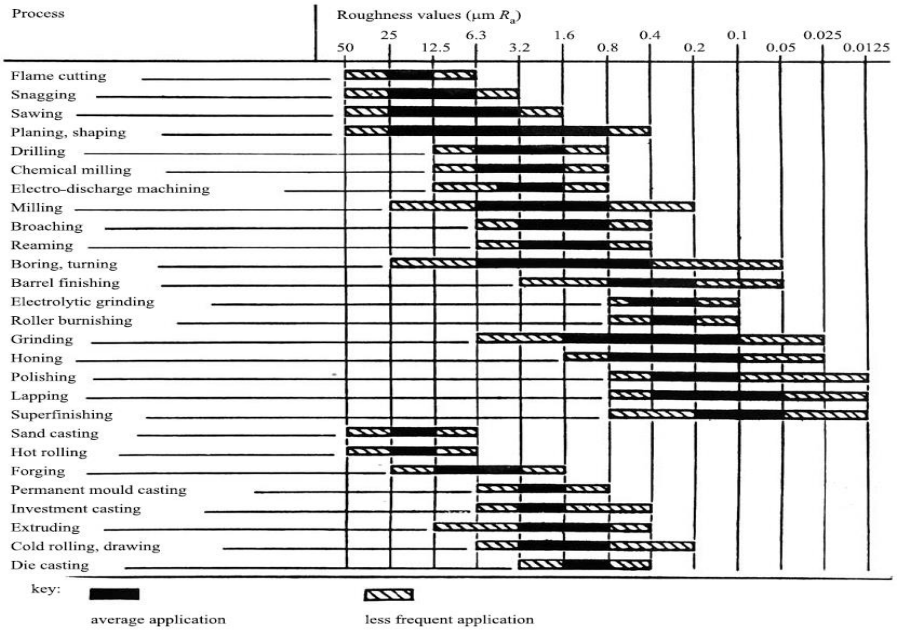

Figure 1.3 Typical surface roughness dimensions resulting from manufacturing processes. Reproduced from (Whitehouse, 2011).

The experimental work described in this work focuses specifically on the measurement (also called *profiling*) of the **surface roughness** and the **step height** of a test material as determined by a contact (mechanical) technique and by a non-contact (optical) method – the lay and waviness of the material were not investigated and so will not be referred to further in the report.

1.2.3 Describing roughness

There is no shortage of descriptive parameters that have been developed to describe the roughness of a surface. This report will highlight those most relevant to the experimental work conducted. For a more complete discussion of the full range of parameters, see for example (Gadelmawla et al., 2002) or refer to the copy of the ISO 25178-2:2012 standard (ISO25178, 2012) that is available at the ISO web site (http://www.iso.org).

1.2.3.1 Amplitude parameters

A number of different diagnostic two-dimensional amplitude parameters are defined with regard to height variation measurements on material surfaces made with respect to a given reference level. These parameters are summarized in Figure 1.4 below.

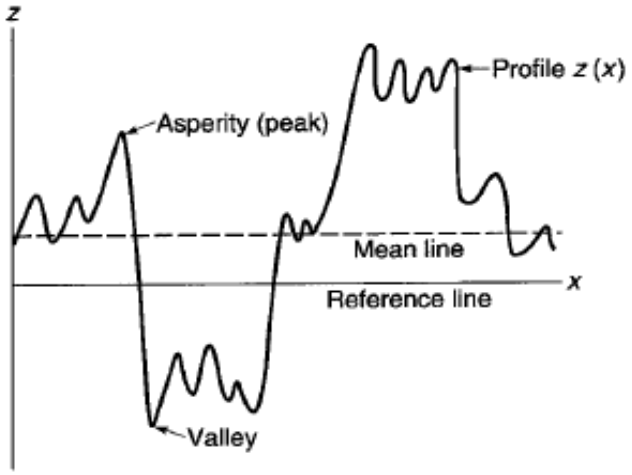

Figure 1.4 Schematic of a surface roughness profile indicating the key features from that amplitude parameters are defined and determined. Reproduced from (Bhushan, 2001).

These include the arithmetic (or center line) average height (R_a), and the maximum peak to valley height (R_z). These are the roughness parameters reported in the experimental section. Other height parameters include root mean square height (R_q), maximum valley height (R_v) and maximum peak height (R_p) (Bhushan, 2001). They can be useful, but since they were not measured in this work, they would not be discussed further.

Arithmetic average height – the mean of a number (n) of absolute height values (z_k) calculated with respect to the mean line through the full profile obtained over a given sampling length (x):

$$R_a = \frac{1}{n}\sum_{k=1}^{n}\left|z_k\right| \tag{1}$$

Ranges of characteristic R_a values provide for a number of standardized roughness grading systems. One of that commonly referred to is the grading number (N). Table 1.1 shows the

maximum R_a value that corresponds to *N1 – N12* that cover the majority of surface textures encountered in material science and engineering applications.

Maximum peak to valley height – the highest peak-mean line height plus lowest valley-mean line height) over the measured sampling length:

$$R_z = R_p + R_v \qquad R_p = \max\{z_k\} \qquad R_v = \min\{z_k\} \tag{2}$$

In this project we used the Japanese Industrial Standard (JIS.30601) definition for R_z, based on the five highest peaks and five lowest valleys over the entire sampling length:

$$R_z^{JIS} = \frac{1}{5}\sum_{m=1}^{5}\left(R_p^{(m)} + R_v^{(m)}\right) \tag{3}$$

Where $R_p^{(m)}$ and $R_v^{(m)}$ are the *m*-th highest peak, and the *m*-th lowest valley respectively.

Table 1.1 Roughness grading numbers and their R_a values. Adapted from (Bhushan, 2001). The higher the *N* number, the greater the roughness of the surface.

Maximum R_a value / µm	Roughness grading number (*N*)
0.025	N1
0.05	N2
0.1	N3
0.2	N4
0.4	N5
0.8	N6
1.6	N7
3.2	N8
6.3	N9
12.5	N10
25.0	N11
50.0	N12

Skewness of the assessed profile – skewness is proportional to the mean cube of the height values recorded. It is an indicator of the asymmetry of the distribution around its midpoint:

$$R_{sk} = \frac{1}{Rq^3}\left[\frac{1}{N}\sum_{k=1}^{N} Z_k^3\right] \tag{4}$$

The value of the skewness determines whether the bulk of the material is located above the middle line (negative values) or below the middle line (positive values). When two surfaces have similar R_a, the skewness parameter provides a way of distinguishing them. Richard Leach provides a good example of the usefulness of the skewness parameter in his Good Practice review: "*A characteristic of a good bearing surface is that it should have a negative skew, indicating the presence of comparatively few spikes that could wear away quickly and relative deep valleys to retain oil traces. A surface with a positive skew is likely to have poor oil retention because of the lack of deep valleys in which to retain oil traces. Surfaces with a positive skewness, such as turned surfaces, have high spikes that protrude above the mean line.* R_{sk} *correlates well with load carrying ability and porosity.*" (Leach, 2001)

Kurtosis of the assessed profile – kurtosis is proportional to the mean fourth power of the height values recorded. It is an indicator of the spikiness / bumpiness of the surface:

$$R_{ku} = \frac{1}{Rq^4}\left[\frac{1}{N}\sum_{k=1}^{N} Z_k^4\right] \tag{5}$$

A spiky surface would have a high value of kurtosis and a bumpy surface a low value. This parameter is useful for predicting surface wear and lubrication properties (Leach, 2001).

1.2.2.2 Spacing parameters

Apart from the perpendicular amplitude deviations used to characterize surfaces, other descriptive parameters have been established to characterize surface details in the parallel direction (Bhushan, 2001; Conroy and Armstrong, 2006; ISO4287, 1997). These include peak density (N_p) - the number of peaks (of any amplitude value) present in a profile per unit length across a surface, and the zero crossings density (N_0) that indicates the number of times a profile crosses the mean line per unit length. The reciprocal of the peak density ($1/N_p$) gives a measure of the average spacing between consecutive peaks and is therefore called the mean peak spacing (A_R).

1.2.2.3 Hybrid parameters

As the name implies, these alternative parameters incorporate a combination of data – that of profile feature height and spacing. Two of the most important parameters of this type are the

average slope and average curvature of a peak or a valley (Bhushan, 2001; Conroy and Armstrong, 2006; ISO4287, 1997). The latter is especially important as its magnitude indicates whether, upon contact from a stylus, a peak on the sample surface would return to its former shape (elastic deformation) or remain distorted (plastic deformation). These parameters were not investigated in the experimental part of the project and so are not discussed in any further detail.

1.3 Surface metrology

In order to accurately characterize any material surface, it is essential to perform measurements from which the key parameters discussed above can be determined – this is the role of surface metrology. In engineering and materials science applications, such metrology is vital for the fine-tuning of a manufacturing process and for determining the functional properties of the surface (Lonardo et al., 2002). These two considerations can be treated separately, but often are inextricably linked in the final goal of producing an accurately tailored surface for a particular application. As constant developments in surface characterization methods are made (Jiang and Whitehouse, 2012), the range of applications of those methods is increased accordingly (Mathia et al., 2011).

A number of instruments and methods have been developed over the past century or so for the measurement of the roughness of a material surface. See, for example, (Jiang et al., 2007a, Jiang et al., 2007b) for a detailed historical timeline of methodological progression to recent times. Broadly, these can be split into categories of contact (‘tactile’) and non-contact ('optical') methods (Sherrington and Smith, 1988a; Sherrington and Smith, 1988b; Whitehouse, 1997). The contact variety employs a mechanical means of determining the surface roughness using a shaped-tip stylus (or a cantilevered arm) that is translated across the surface under investigation and data converted either electronically, as in instruments called *profilometers* (translation in one dimension), or optoelectronically using atomic force microscopes (AFMs, translation in three dimensions).

The experimental section of this report describes roughness measurements conducted using a stylus profilometer. Non-contact methods employ optical phenomena, such as wave

interference – the constructive or destructive superposition of light waves between a reference beam and a second beam reflected from the surface being studied. This report describes the use of the most commonly available method based on this principle known as *white light interferometry* or WLI. Both methods (along with others available) have advantages and disadvantages depending on the precise nature of the material and the specific requirements for data acquisition (Leach and Haitjema, 2010).

Table 1.2 lists some of the *pros* and *contras* of metrology methods currently employed for surface texture characterization, along with key resolution information and operating conditions. A direct comparison of data obtained from the same material surface using more than one method is therefore vital for a detailed assessment of the nature of a particular surface under investigation (Conroy and Armstrong, 2006, Vorburger et al., 2007).

Table 1.2 Key range and resolution features for the main profiling methods used in the measurement of surface texture. Reproduced from (Whitehouse, 1997). Acronyms: TEM – transmission electron microscopy, SEM – scanning electron microscopy, STM – scanning tunneling microscopy.

Method	Spatial resolution	z resolution	Range z	Frequency	Comments
Stylus	0.1 μm to 1 mm	0.3 nm	50 μm	20 Hz	Contacts workpiece; easy to use; traceable
Optical probe	0.5 μm	0.1 μm	20 μm	10 Hz to 30 kHz	Non-contacting; less traceable; with servo drive; range extended to 50 μm
Heterodyne	2.5–200 μm	0.2 μm	0.5 μm	10 Hz	Requires computer unravelling
TIS	0.6–12 μm	1 nm	0.1 μm	Seconds	
Scatterometer diffraction	$\simeq$ 10 μm	1 nm	$\lambda/8$ 100 nm	Seconds	Resolution depends on aperture; insensitive to movement
TEM	2 nm to 1 μm	2 μm	100 nm	Minutes	Replication needed can destroy surface
SEM	10 nm	2 nm	2 μm	Minutes	Vacuum needed
STM	2.5 nm	0.2 nm	100 nm	Minutes	Vibration-free mounting
Normarsky	$>$ 0.5 μm			Minutes	Needs interpretation and certain minimum reflectivity
Capacitance	2 μm	1 nm	50 nm	2 kHz	Needs conductors
Interferometry	2 μm	1 nm	1 μm	Minutes	

1.4 Objectives of this work

The primary aim of the experimental work conducted and described in this thesis is to critically evaluate two measuring techniques (WLI and Stylus instruments) for the surface profiling of step *height* and *roughness measurement* and to find the best measuring method approach to establish an optimum way of determining *step height* (using quartz glass substrate) and *roughness* (using tungsten substrate) parameters. A number of methods have been developed

for such a purpose in engineering applications and the disciplines of the materials and surface sciences. However, each is subject to its own inherent operational advantages and disadvantages and, to varying degree can be dependent upon the nature (composition and physical/chemical properties for example) of the surface. Consequently the choice of technique for a particular measurement is vital for an accurate description of the sample surface.

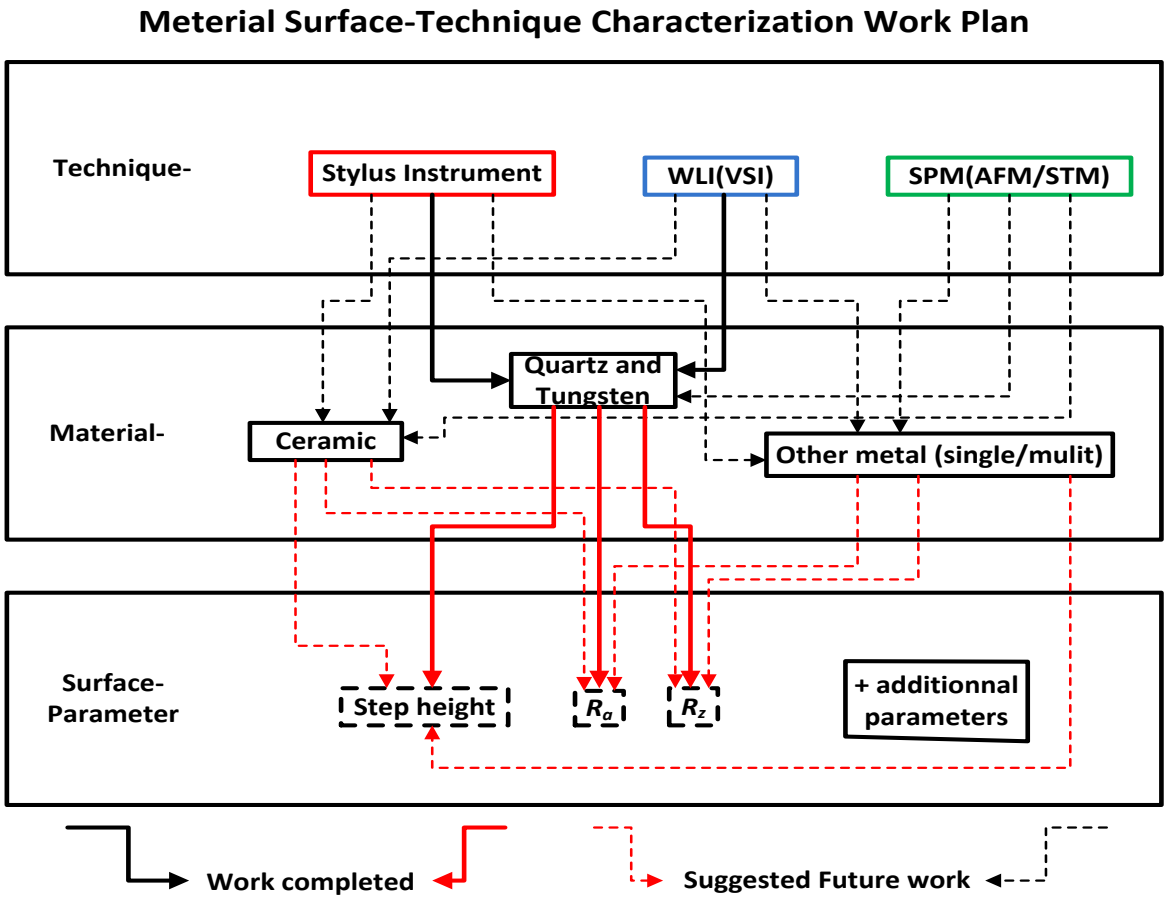

Figure 1.5 Work plan schematic apply in the experiment.

The **first objective** concerns the nature of the experiment itself: to assess the practicality and versatility of two commonly used methods of surface characterization:

(1) A *contact* method of stylus profilometry

(2) A *non-contact* method of white light interferometry

for surface profiling of the same substrate.

The **second objective** concerns the analytical treatment of the data generated: to collate and graphically represent the data from both methods in a clear and informative manner in order to best reflect the repeatability of each data set acquired from a number of different positions on the substrate surface.

The **third objective** concerns the critical analysis and conclusions drawn: to compare the final data values produced by both methods with the nominal values given for the reference surface used, and to investigate the reasons for any differences between the values produced by the two measurement methods.

Chapter 2

2. Measurement methods

2.1 Contact method – the stylus profilometer

Stylus-based instruments are the most common tools for measuring surface texture. A stylus profilometer works by tracing the surface with a sharp tip (“stylus”) and recording the tip position using optical or electromechanical methods (Conroy and Armstrong, 2006). A stylus instrument contains a stylus that contacts the surface and an electromechanical transducer that converts its Z coordinate into voltage, followed by an amplifier that makes that voltage easier to digitize, followed by an analogue-to-digital converter that is connected to a computer (Leach, 2001).

The tip of the stylus is usually made of diamond with a carefully calibrated profile. Because the stylus tip is a finite object, it cannot trace the surface perfectly and essentially gives a "filtered" image of the surface. For this reason, high frequencies in the surface profile would be more affected by the stylus shape than the low frequencies. The effect of the stylus force is also important – if the force is too high, the surface may be damaged. If the force is too low, the stylus would not trace the surface with sufficient accuracy (Leach, 2001).

2.1.1 Profilometer components: stylus

At the heart of the surface profilometer lies the stylus that makes direct contact with the surface under study. As the stylus is displaced across the surface, moving relatively at a constant speed (either stylus or surface can be chosen as the stationary object), its vertical motion (temporal displacement from a starting rest position) is amplified via a transducer such as a coupled linear variable differential transformer (LVDT) or sensor and digitally converted for imaging and subsequent analysis by instrument software (Guo et al., 2013; Lee and Cho, 2012; Clark and Greivenkamp, 2002; Morrison, 1995).

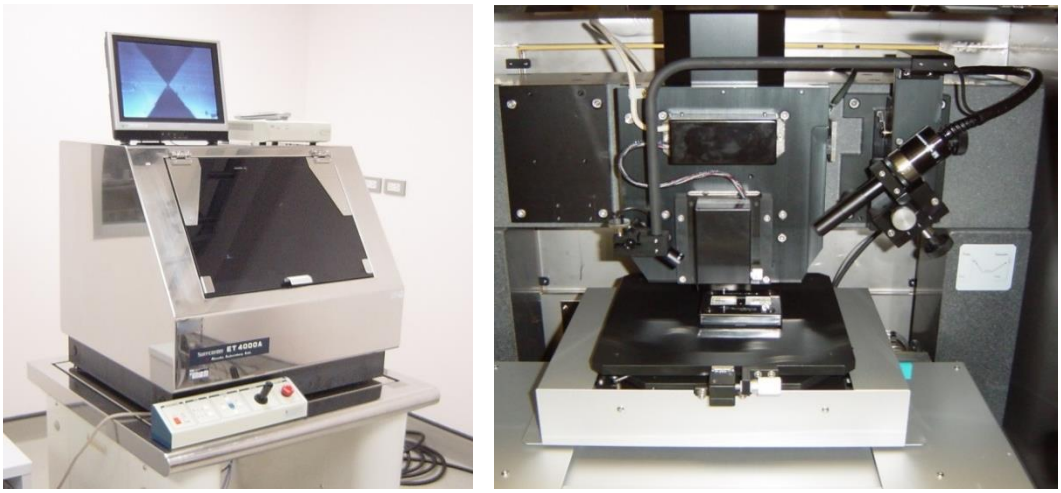

Figure 2.1 The stylus instrument used to measure surface parameters in this study.

Invariably, tested surfaces are 'hard' in nature (*e.g.* metals, alloys and ceramics), that necessitate the stylus to be composed of a robust, indestructible material – most commonly diamond but other types, such as sapphire or ruby (both forms of aluminum oxide – Al_2O_3), or in the case of 'softer' surfaces (*e.g.* polymer), a silicon nitride (Si_3N_4) tip, are often employed. Different stylus geometries and tip dimensions have been developed within the range of instruments currently commercially available for application in industrial settings or academic research laboratories (*e.g.* surface science disciplines). The most frequently deployed form of stylus has a conical shape with a rounded (contact) edge typically characterized by a cone angle of 60 degrees and a 2 µm radius (Lee and Cho, 2012). This arrangement is shown schematically in Figure 2.2 below.

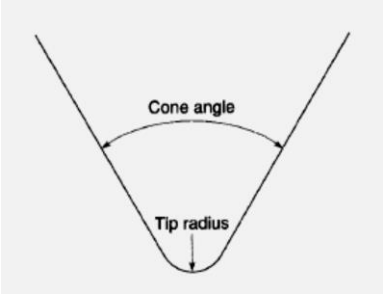

Figure 2.2 Cone-shaped stylus with key geometric features of tip radius and cone angle indicated. Reproduced from (Bhushan, 2001).

Styli are also frequently made in an asymmetrical pyramid shape (dimension a < b – see Figure 2.3) that confers additional strength to the stylus structure in response to any induced shock as it traverses the surface. It also helps to lower the pressure exerted on the surface. The smaller dimension ('a') is always kept at the right angle to the direction of movement of the stylus. For an isotropic surface (one that is essentially uniform in all directions), the crucial dimension for the stylus will be the larger one (‘b’) and generally will be significantly larger (compared to a typical cone-shape) at 7 or 8 µm that necessarily reduces the resolution of the surface details. This resolution reduction is known as *integration* (Guo et al., 2013; Lee and Cho, 2012; Clark and Greivenkamp, 2002; Morrison, 1995).

Figure 2.3 Pyramid-shaped stylus (geometry shown to the right). Image reproduced from (Whitehouse, 2000).

Both of these stylus geometries can suffer from wear with repeated use with cone shapes experiencing ‘flattening’ at the curved contact edge and pyramid shapes suffering from edge smoothing with time. For very finely detailed surfaces (nanoscale), greater data resolution is required and often a cone shape stylus with a smaller slope angle (down to 45 degrees) is employed in order to minimize loss of data as a result of integration (Bhushan, 2001; Whitehouse, 2000).

2.1.2 Profilometer components: skid

Skid contact systems are further classified into two main types (*skidded* and *skidless*) according to the precise nature of the contact between stylus and surface. The skidded variety has the stylus contained within the body of a probe consisting of a metal component (skid) that contacts the surface under study. In this configuration, the surface acts as its own reference. The skid is usually either ‘button-like’ (positioned in front or behind the stylus) or ‘doughnut-

like' in that the stylus extends through a central hole. The skidless form is comprised of an 'internal' surface that acts as the reference and generally allows for a greater range of surface texture characteristics in addition to the roughness (Bhushan, 2001, Whitehouse, 1997, Whitehouse, 2000, Whitehouse, 2011).

One particular issue to bear in mind with the button-like skid-probe system is illustrated in Figure 2.3 below. The skid must be 'blunt' enough in order to adequately span adjacent peaks in the surface roughness (Figure 2.4a) and not suffer from significant 'drop' into valley structures (Figure 2.4b).

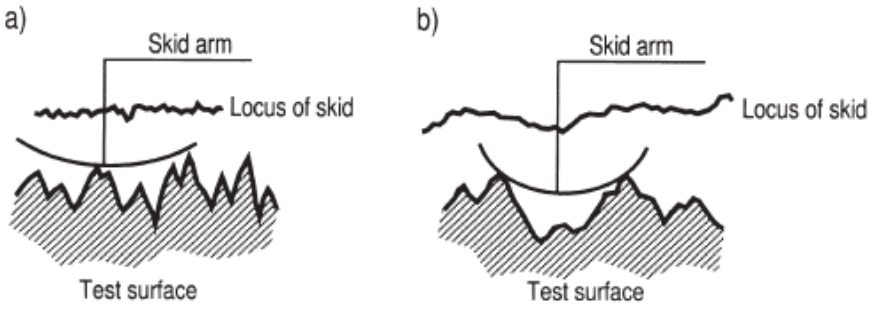

Figure 2.4 Skid geometry schematic – reproduced from (Whitehouse, 2000).

2.1.3 Profilometer components: gauge

The gauge system is the critical link in the transfer of vertical motions from the stylus through its connecting arm as it traverses the surface, to the instrument electronics that convert these displacements into digitized data. The stylus arm–gauge configuration is essentially a classical spring-mass system (see Figure 2.5) that controls the tracking force exerted between the stylus tip and the surface it is contact with (Bhushan, 2001; Whitehouse, 1997; 2000; 2011).

As with any such spring-mass system, the gauge has a characteristic resonant frequency of vibration of a few hundred cycles per second or Hertz (Hz). It is therefore an essential requirement to ensure that the measurement frequency (controlled by the speed at that the stylus is moved relative to the surface) is maintained significantly below this resonant frequency at all times in order to avoid unwanted resonance effects (Bhushan, 2001; Whitehouse, 1997; 2000; 2011).

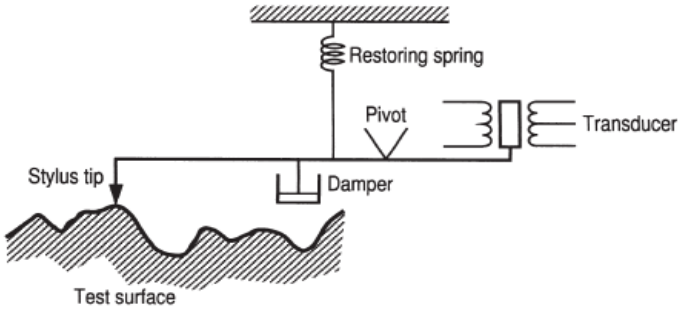

Figure 2.5 Stylus-transducer coupling – reproduced from (Whitehouse, 2000).

The most common gauge type is of the inductive type, known as a linear variable differential transformer or LVDT (Figure 2.6). Stylus movement is translated through the arm and produces the movement of a ferrite core inside a transformer that forms part of an AC bridge circuit. A resulting difference in signal within the bridge is proportional to the core displacement and therefore to the stylus motion.

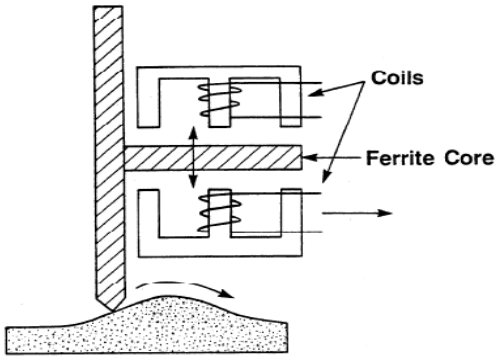

Figure 2.6 Schematic showing the components and basic operating principle of a commonly used transducer, the linear variable differential transformer (LVDT), found in stylus profilometers, and coupled to a stylus traversing a surface – image reproduced from the NIST web site (http://www.nist.gov).

2.1.4 Profilometer components: electronics

The gauge output is first demodulated and amplified and then converted to a digital signal for computerized storage and analysis. Prior to the signal conversion process, an anti-aliasing another filter is often utilized to ensure that the frequencies from the stylus are within the operational range of the system *i.e.* below the Nyquist threshold (Leis, 2011). In some

instruments, another type of electronic filter, known as a 'sample and hold', is employed to ensure no loss of the analog signal prior to conversion to digital form (Diniz et al., 2010). Figure 2.7 shows the major electronic stages coupled with the other components within a modern stylus profilometer.

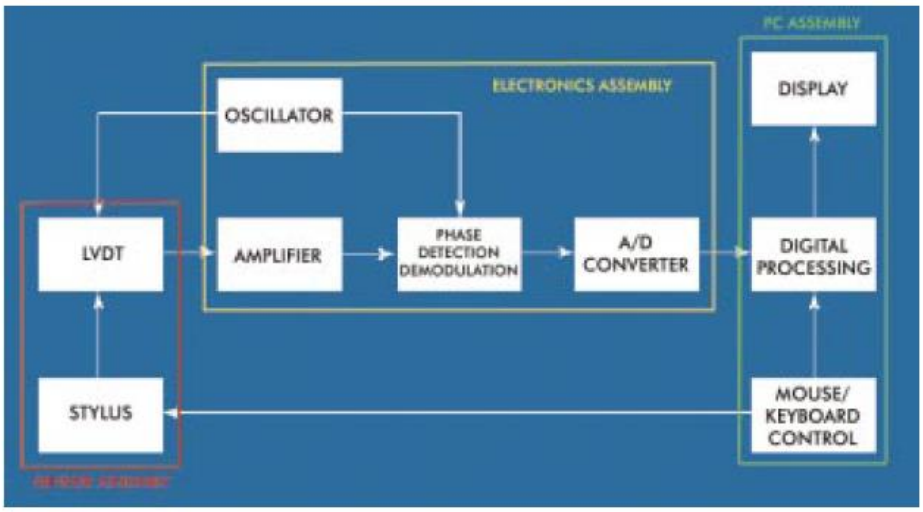

Figure 2.7 Key components (stylus, electronics, PC) of a modern stylus profilometer. Image reproduced from the Veeco Metrology Group web site (http://www.veeco.com).

2.1.5 Measurement considerations

The most commonly used styli have radii of 2, 5 and 10 µm and a 90 degree angle. The radius of the stylus tip determines the force of contact with the surface. The smaller the radius, the lower the force required *via* the gauge system. If the force is exceeded in this case, irreversible scratching of the surface can result. Typical contact force levels used range between around 0.7 to 15 mN for 2 – 10 micron radii styli, although smaller tip sizes and lower forces have also been reported as practical means of achieving increased resolution for surface profiling (Song and Vorburger, 1991).

Within the skidded gauge instruments, the button-like skid can be prone to certain measurement limitations – for example, on relatively rough or wavy surfaces, this type of skid can suffer from 'riding' whereby it can temporarily lose contact with the surface detail within a peak-valley geometry and adversely affect the distance between contact and reference. As a result, data is likely to be unreliable or of low repeatability. In contrast, the design/geometry of

the doughnut-like skid largely overcomes this problem, maintaining contact at all times and therefore presenting a more constant reference surface for accurate measurement. Conversely, the structure of the donut-like skid means it is not suited to certain surface types and therefore careful consideration of surface type with regard to the precise gauge (and tip) should be given before surface roughness measurements are taken (Bhushan, 2001; Sherrington and Smith, 1988a; Song and Vorburger, 1991).

All of the inherent signal filtering processes and stages described above impose a range of instrument output frequencies that are linked to the spatial frequencies on the surface under investigation by the speed at which the stylus is moved in relation to the surface. Consequently, depending on the nature of the surface, key operational considerations are the tip dimensions and the rate of traverse. For example, for measurement of a fine surface finish, a sharp stylus (to maintain contact at all times) and comparatively slow stylus speed (to ensure effective surface tracking and control of resulting frequencies within the bandwidth of the electronics) is essential. In such cases typical measurement stylus speeds are of the order of 0.25 – 1 mm/s (Bhushan, 2001; Sherrington and Smith, 1988a; Song and Vorburger, 1991).

2.1.6 Limitations and potential sources of error

The finite dimensions of any stylus tip can lead to the distortion of a surface profile to some degree as illustrated by Figure 2.8. Whilst the magnitude of peak curvature can be exaggerated, a valley feature may show up in the profile as an abrupt cusp. These effects are particularly pronounced for peaks and valleys with a radius of curvature of a micron or less, with a number of very steep sloped features with angle greater than 45 degrees (Mccool, 1984).

A further potential error source inherent in the contact stylus instrument is possible ‘lift-off’ of the tip as it traverses a surface as a result of its scanning velocity being too high for a particular surface type or specific area on a given surface. Such an eventuality is essentially determined by factors including not only the local geometry of the surface but also the ratio of the spring restoring constant to the attached stylus mass (Pawlus and Smieszek, 2005).

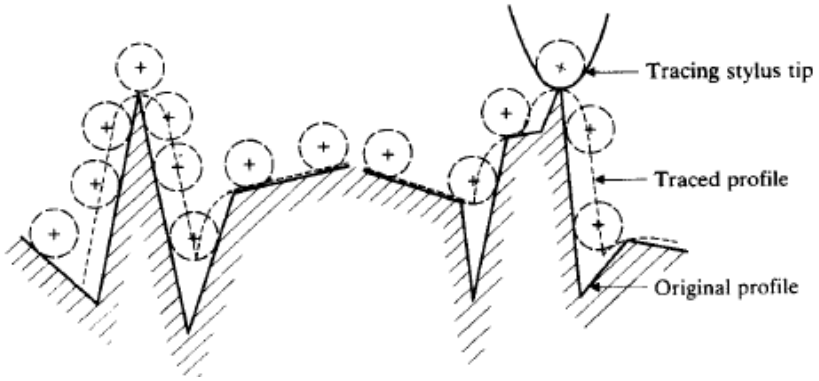

Figure 2.8 Illustration of the potential distorting effect at peaks and valleys on a surface profile due to the finite-sized stylus tip. Reproduced from (Bhushan, 2001).

Further, the stylus load is also a possible error source. If the load is too great, the resulting high pressure it may exert over the very small contact area on the surface can produce an undesired distortion (elastic deformation) at this point. If such a load exceeds the intrinsic material hardness, this deformation can become a plastic type leading to permanent damage at the surface and compromise profiling of the material. Also scratches left by a stylus will cause permanent damage and lead to measurement error. This is particularly true for metallic samples (Arvinth Davinci et al., 2014).

Clearly, it is important to parameterize any stylus dimension, speed and load in any surface profiling experiment in order to minimize the possibility of any of the error sources discussed above from compromising the data accuracy and spoiling the sample itself. See, for example, (Arvinth Davinci et al., 2014; Mccool, 1984; Pawlus and Smieszek, 2005) for practical and theoretical discussions of some of these influencing factors.

2.2 Non-contact method – the white light interferometer

The interferometric method of surface profiling uses the wave-like nature of light to accurately measure distances. The fundamental principle behind interferometric instruments goes back to Michelson and Morley (Michelson and Morley, 1887), who had observed a pattern of fringes after sending identical beams of light along slightly different paths.

2.2.1 Light interference phenomenon

The fundamental physical principle underpinning all optical interferometry methods and instrumentation is that of interference – the superposition of two electromagnetic waves that are either in-phase or out-of-phase. The in-phase superposition results in constructive interference (whereby the resulting wave is enhanced in amplitude compared with each individual component), whilst out-of-phase superposition produces destructive interference (the resulting wave is diminished in amplitude compared with each individual component) – see Figure 2.9. When the result is viewed on a screen or through a microscope, a pattern of light and dark fringes is observed due to the constructive and destructive interference effects respectively (Sherrington and Smith, 1988b).

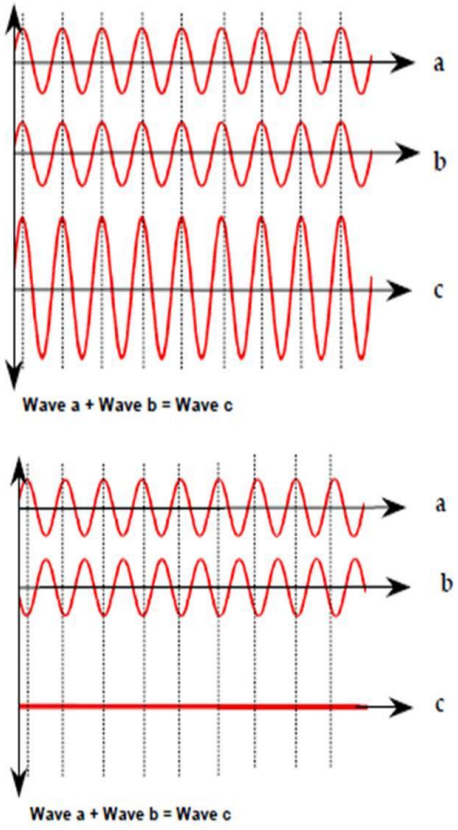

Figure 2.9. Schematic illustration of constructive (top) and destructive (bottom) wave interference. Reproduced from the NPL web site (http://www.npl.co.uk).

There are a number of different optical configurations for specific interferometers, but the basic components of any such instrument include (Hocken et al., 2005):

1. A light source, either monochromatic or broad-band;
2. A beam splitter, usually a cube comprised of two triangular prisms (this was the arrangement in the original Michelson interferometer) to split the light into a reference beam and a measurement beam;
3. An optical system – a combination of lenses and mirrors with an aperture – to recombine and focus the two beams;
4. A digital sensor, such as a charge-coupled device, that converts the light intensity pattern into the digital form.

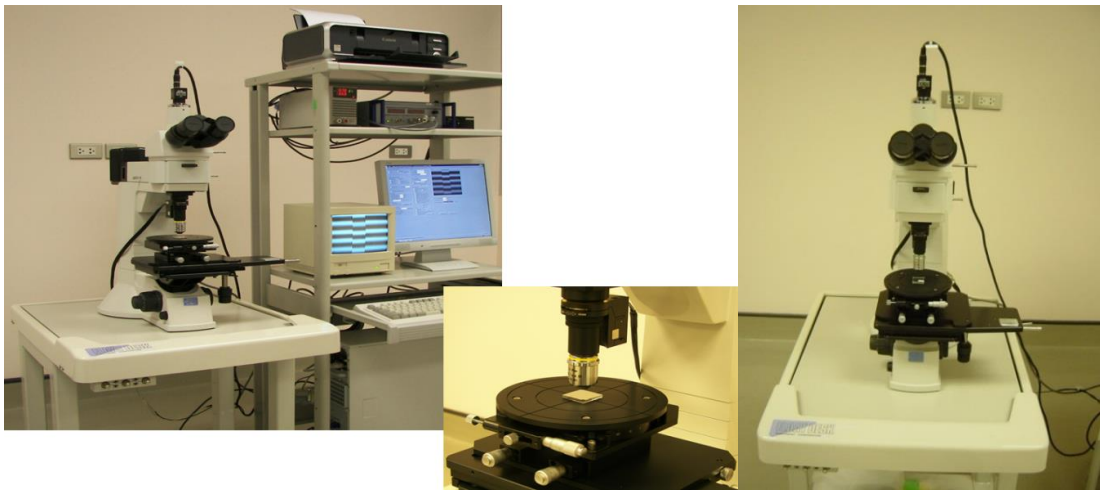

Figure 2.10 The VSI instrument used to measure surface parameters in this study.

Figure 2.11 shows the schematic of the basic structure of a more recently developed instrument called a *Mirau interferometer* that is commonly used for surface analysis, including the step height and surface roughness. The classic Michelson type also shown differs primarily in the position of the reference surface (Hariharan, 2003). In the Mirau-type interferometer, the initial light beam is split by the beam splitter with one beam passing to the reference mirror and the other to the test surface. Both are reflected back and combined at the objective lens of a microscope and then CCD detector where the resulting interference pattern is created.

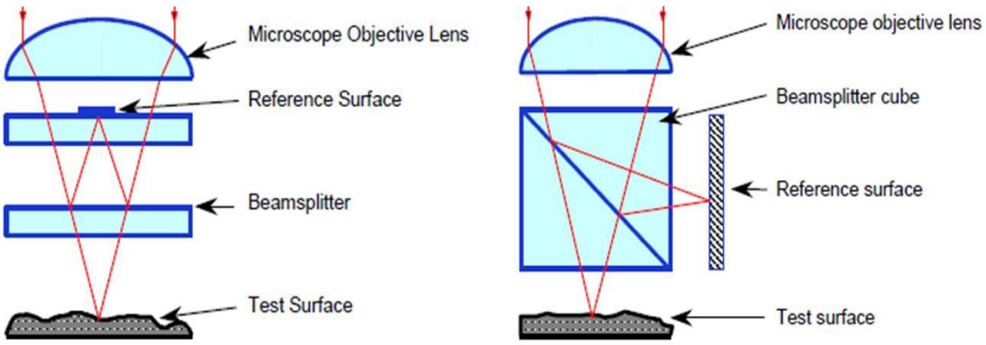

Figure 2.11 Schematic of a Mirau (left) and Michelson (right) interferometer – images reproduced from the NPL web site (http://www.npl.co.uk).

The choice of light source is determined by its wavelength distribution, by the coherence length, the luminous power required and the length of time for which the light source is expected to be in operation. Visible light sources are the most popular because of difficulties with alignment and atmospheric absorption at both shorter and longer wavelengths. In particular, the light-emitting diodes are becoming popular because of the ready availability of multiple wavelengths, reasonable coherence length and also their ability to work in pulsed mode with a short (tens of nanoseconds) response time that enables stroboscopic measurement. However, the applications where large luminous intensities are required still use tungsten halogen lamps. In any case, to enable good VSI measurement, the coherence length of the light must be greater than twice the vertical amplitude difference measured – this ensures the absence of 2π phase measurement artefacts that are described in detail below (Leach, 2008).

2.2.2 Phase shifting interferometry

PSI is a well-established technique that enables 3D imaging of surfaces with very high resolution and repeatability. It relies on the sequencing of images (fringe pattern shifts) that have an accurately controlled phase change between. This sequencing is usually controlled by mechanical manipulation of the interference objective. This form of optical interferometry was not used in the experimental part of the project and so only brief background details will be outlined here (Hariharan, 2003; Hocken et al., 2005; Vorburger et al., 2007).

For a monochromatic light source, the difference in height for two consecutive data points must meet the condition of being smaller than one quarter of the light wavelength or λ/4. This condition necessarily imposes a limited dynamic range for PSI. If the difference is greater than λ/4, then artifacts in the height profile will be introduced with order of nλ/2, where n is an integer. To overcome such a situation, one method that has been developed within the PSI technique uses two incident wavelengths for subsequent subtraction of the desired information. Careful selection of two or more such operating wavelengths will therefore significantly expand the dynamic range of the instrument for step height measurements (Creath, 1987). However, for measuring surface roughness details, a broadband (multi-wavelength) technique such as VSI is a more practical solution although other limiting issues (for example, that of 'skewing') in any optical method must be considered carefully in step height and surface roughness studies (Rhee et al., 2005).

2.2.3 Vertical scanning interferometry

VSI is a type of 'low coherence' interferometry where the underlying principle is that light interference is a product of path-length differences between reference and measurement beams that closely match the coherence (the average correlation between wave amplitudes over a given time delay) of output light from the source. Figure 2.12 shows a typical VSI instrument arrangement. The system measures the intensity of the light as a degree of fringe modulation, or coherence, instead of the phase of the interference fringes. Light from the source is directed upwards by the upper beam splitter to the objective lens (shown below the sensor in the figure) and downwards by the lower beam splitter towards the surface under study. In the latter case, the beam is then further split into one beam that is incident on the sample surface and another that is incident on the internal reference mirror. The two beams are then subsequently recombined and passed back up to the detector (*e.g.* a CCD). The stated coherence criteria for this technique means that the difference in optical path length traversed by the two beams must be close enough to result in the desired interference pattern (Conroy and Armstrong, 2006; Conroy and Mansfield, 2008; Hariharan, 2003; Hocken et al., 2005; James, 1995).

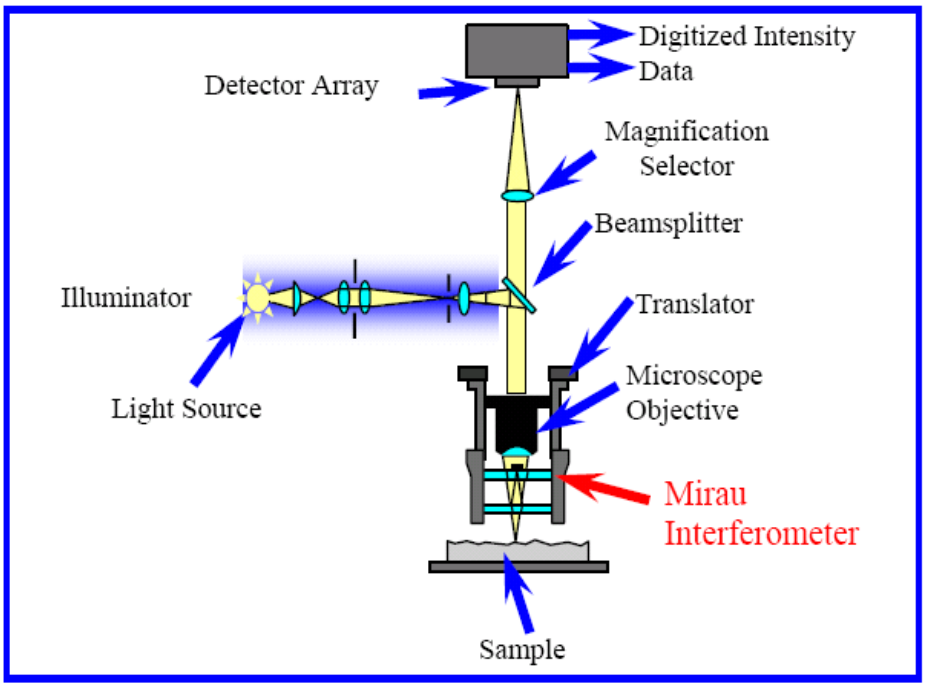

Figure 2.12 Schematic of a modern vertical scanning interferometer – image reproduced from (James, 1995).

The fringe contrast is translated through focus at the single sample point, as illustrated in the Figure 2.13. The images output acquired from CCD array are calculated by commercial software on computer. Figure 2.14 shows the schematic diagram of the white light interferometry system.

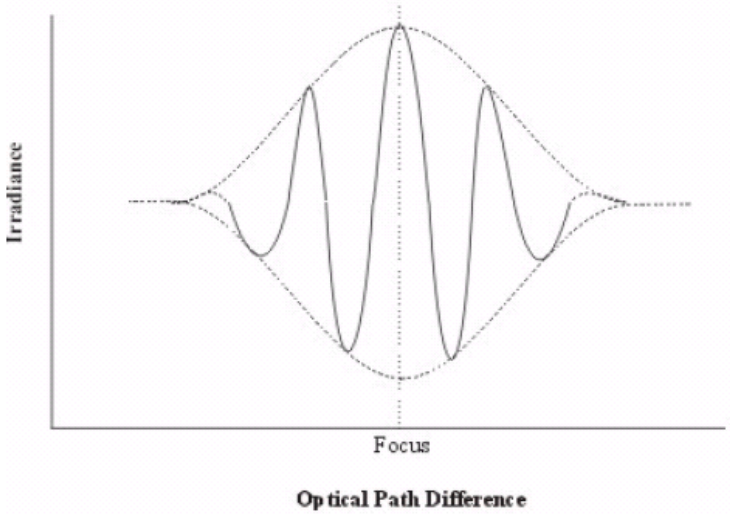

Figure 2.13 The fringe contrast is translated through focus at the single sample point– image reproduced from (James, 1995).

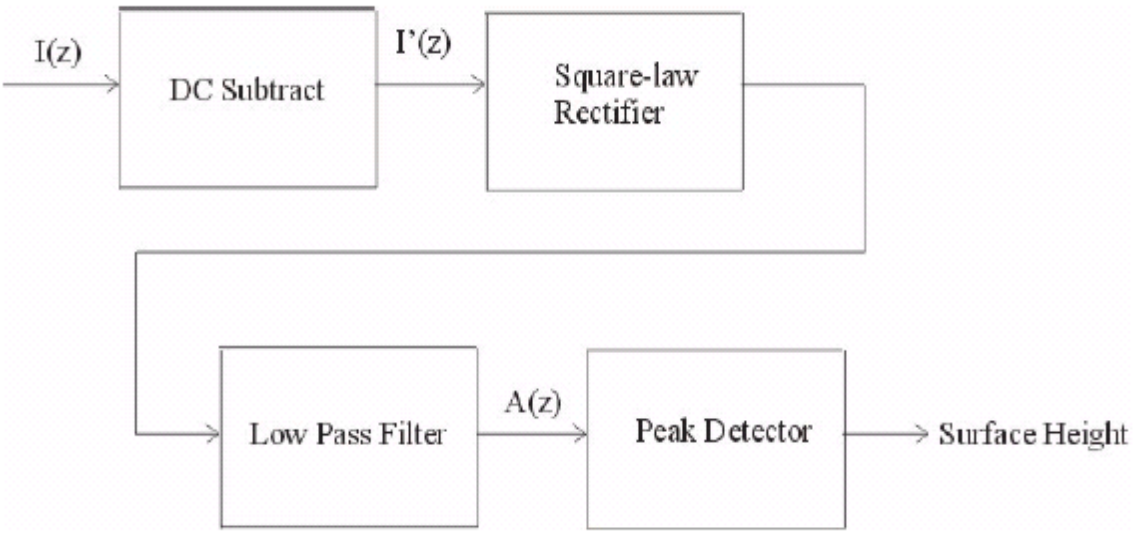

Figure 2.14 The schematic diagram of the white light interferometry system.

One key operational factor is the numerical aperture or NA. This a dimensionless number that denotes the spread of incident angles over that light can pass through the objective lens of the instrument. Figure 2.15 is a schematic showing the critical acceptance angle (α) such that:

$$NA = n \sin \alpha \tag{6}$$

where n is the refractive index of medium (for air, n = 1 and 0 < NA < 1).

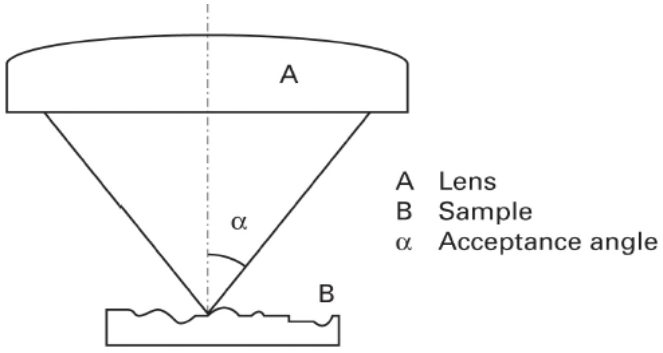

Figure 2.15 Illustration of the acceptance angle within a VSI instrument from that the numerical aperture is defined – image reproduced from the NPL web site (http://www.npl.co.uk).

VSI has become increasingly popular for detailed surface studies due to a number of key factors such as (Hariharan, 2003, Hocken et al., 2005):

- High resolution
- High repeatability
- High quantitative accuracy
- Non-destructive character – no contact is made with the surface
- Possibility of full automation
- Fast operation and relatively simple sample loading and preparation
- Flexibility in terms of the range of materials that can be studied
- Ability to measure both roughness and step height simultaneously.

Because of this versatility and accuracy, the VSI technique was the non-contact profiling method selected for use in the experiments to measure the sample surface roughness and step height that are described later in this report.

2.2.4 Processing of interferometric data

Surface profile data may be extracted from interferometric profiles in several ways. Currently the most popular methods include the measurement of the modulation envelope and light phase estimation, or some combination of the two. As it happens with all inverse problems in physics, the reconstruction problem is mathematically ill defined and, unless special measures are taken, the resulting surface topography would be a strong function of the artefacts (optical aberrations and dispersion, surface tilt, multiple scattering effects, electronic noise, *etc.*) in the primary data. It is therefore necessary to use robust data processing methods that are stable with respect to minor perturbations in the primary data (Bhushan, 2001).

2.2.4.1 Envelope detection

Envelope detection relies on the measurement of the *envelope* of the light intensity modulation rather than the full signal. Envelope may be obtained by either demodulating the signal at the fringe frequency electronically or by numerically Fourier transforming the signal and shifting the frequency peak to zero frequency, followed by the inverse Fourier transform. Envelope

detection is more robust than peak value estimation for surface height measurement because it requires less instrumental stability. Fitting the envelope curve is also mathematically more robust because the number of least squares minima in the envelope fitting process is much smaller than that for the full modulation curve. Envelope maximum position is also less sensitive to the instrumental noise – the primary advantage here is that the numerical differentiation operation (which is ill-defined for noisy data) is replaced by the integration operation, which is always well defined. The resulting interference is recorded by the CCD camera in the white light interferometry. The resulting interference light intensities corresponding to phase-shifting step of 0, $\pi/2$, π and $3\pi/2$ are assigned as *A(x, y)*, *B(x, y)*, *C(x, y)* and *D(x, y).* These intensities can be acquired by moving the reference mirror through displacements of $\lambda/8$, $\lambda/4$ and $3\lambda/8$, respectively (Haviharan, 2007). The resulting intensities can be written as:

$$A(x,y)=I1(x,y)+I2(x,y)\cos\alpha(x,y) \qquad (1)$$

$$B(x,y)=I1(x,y)-I2(x,y)\sin\alpha(x,y) \qquad (2)$$

$$C(x,y)=I1(x,y)-I2(x,y)\cos\alpha(x,y) \qquad (3)$$

$$D(x,y)=I1(x,y)+I2(x,y)\sin\alpha(x,y) \qquad (4)$$

where $I_1(x,y)$ and $I_2(x,y)$ are two overlapping beams at two symmetric points on the reference surface and the test respectively. The phase map $\varphi(x, y)$ of a sample surface will be obtained by the relation:

$$\phi(x,y)=B(x,y)-D(x,y)A(x,y)-C(x,y) \qquad (5)$$

Once the phase is determined from a two-dimensional CCD array across the interference field pixel by pixel, the surface height distribution/contour, *h(x, y)*, on the test surface can be obtained by

$$h(x,y)=\lambda 4\pi\phi(x,y) \qquad (6)$$

2.2.4.2 Phase estimation

The phase of the electromagnetic wave is determined by the path difference between the two beams of interferometer and (when non-negligible) the refractive index of the surface, expressed as a complex number (so that a phase rotation is incorporated as well as the change in the direction of the wave). Phase estimation method is the most popular data processing method in 3D optical profilometers (Bhushan, 2001; Conroy and Armstrong, 2006; Hariharan, 2003).

A significant limitation of the phase detection method stems from the fact that phase is a periodic function that is only uniquely defined in the $[-\pi, \pi]$ interval. Therefore, the phase estimation method is only useful when the surface height values are less than half the effective wavelength. When the deviation is greater than that, the phase would loop back into the same interval and complicated unwrapping methods must be used to recover the surface profile. Unwrapping, however, relies on the assumed continuity of the surface and therefore the interferometric profilometry methods might not be applicable to extremely spiky surfaces because the amplitude of the spikes might be under-estimated *via* incorrect unwrapping. Ideally, interferometric methods should therefore be used for very smooth surfaces.

Fringe analysis and phase unwrapping can be automated to a significant extent using, for example, the *integrating bucket method* (Bhushan, 2001) in which the phase difference between the test and the reference surface is analyzed automatically by a computer. The lack of need for manual phase unwrapping is a major advantage because it saves the operator time and permits the use of less skilled (and therefore cheaper) operators.

2.2.5 Limitations of vertical scanning interferometry

VSI has a number of well-documented distortion problems that must be accounted for in high-precision measurements. Those problems are listed in this section.

2.2.5.1 Ghost steps and field-dependent dispersion

Ghost steps are apparent steps reported when measuring perfectly flat objects. These steps are created when there is 2π phase jump due to a surface height error of approximately half the wavelength. Phase errors of this type are called 2π errors – error arises from a field-dependent

dispersion that is inherent in the geometry of some interferometers. The ghost steps only appear when phase information is combined with coherence information (Leach, 2008).

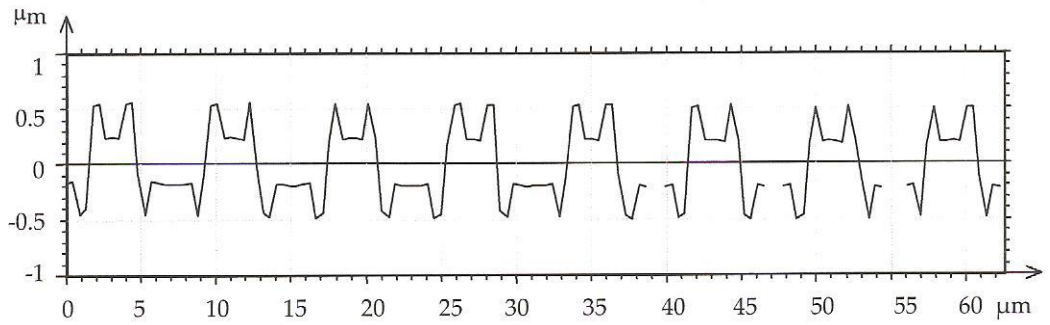

Figure 2.16 Schematic illustration of the field-dependent distortion of a sinusoidal shape. Reproduced from (Niehues et al., 2007).

The cause of such unwanted features is the inherent dispersion effect resulting from the optical configuration within VSI instruments (Niehues et al., 2007). Field-dependent dispersion in general results from sensitivity to the gradient of a surface and produces false signal shapes superimposed at regular intervals (2π) on the underlying sinusoidal form (Lehmann et al., 2014).

2.2.5.2 Batwing effect

This type of error (named after the characteristic shape it creates) arises in proximity to step features where the step height is smaller than the coherence length of the light source.

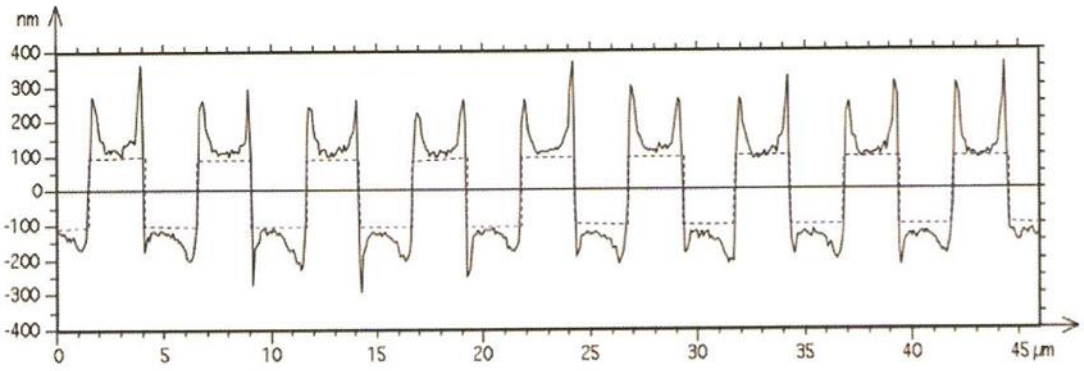

Figure 2.17 Schematic illustration of the ghost batwing effect. Reproduced from (Gao et al., 2008).

It is caused by wave reflections from top and bottom surfaces of a sample (Gao et al., 2008) and observed around step discontinuities particularly when a step height is less than the coherence length of the incident light. VSI does not yield correct surface height near the step even if the step height is greater than the coherence length – this effect must be taken into account when measuring a step height artefact to calibrate the instrument. It is not expected to be observed for smooth samples.

2.2.5.3 Multiple scattering and phase errors

In general, it is found that the surface roughness of a sample tends to be over-estimated by VSI compared with other methods. This is primarily attributed to the diffraction and dispersion effect, which cause deviations between surface height values obtained from the white-light interferometer.(Lehmann et al., 2014; Niehues et al., 2007).

The optical properties of the material surface under study can also give rise to unwanted effects. For a multi-component material, different phase changes for different materials can result upon reflection that can corrupt surface height determinations (Hariharan, 2003; Hocken et al., 2005). Phase changes are usually less than 45 degrees (corresponding to height errors of less than 30 nm), but they can contribute to the 2π errors described above (Leach, 2008).

2.3 Other surface profiling methods

Although the stylus and the interferometry methods described above are the longest established means of measuring a surface texture and characterizing its roughness, a number of other methods have found increasing application to achieve such goals. Although these were not used in the experimental part of this project, for completeness a brief background is now given on the most popular of such 'alternative' methods of atomic force microscopy (AFM) and scanning tunneling microscopy (STM). Both of these are classed as variations of *scanning probe microscopies* and are capable of resolving surface features down to much lower spatial scales (nanometers) and producing highly detailed 3 dimensional representations of the surface under investigation (Danzebrink et al., 2006).

2.3.1 Atomic force microscopy

Figure 2.18 depicts the main components of an AFM instrument. The point of contact with a surface is made by the tip that is able to measure extremely small forces (nanonewtons) through the displacement of the connecting cantilever arm (most commonly composed of silicon or silicon nitride) as the tip is scanned by the translator (xyz) stage and traverses the surface underneath it (Bhushan, 2001). These displacements are detected by laser reflection from the cantilever to a deflection sensor such as a photodiode array. Depending on the precise application and nature of the sample, the AFM instrument can be run in different modes: *contact* mode where the tip is physically moved over the sample surface, *tapping* mode where the tip oscillates at or near to its resonant frequency just above the surface, and *non-contact* mode where the tip is scanned close to, but without coming into contact with a surface (Danzebrink et al., 2006, Poon and Bhushan, 1995).

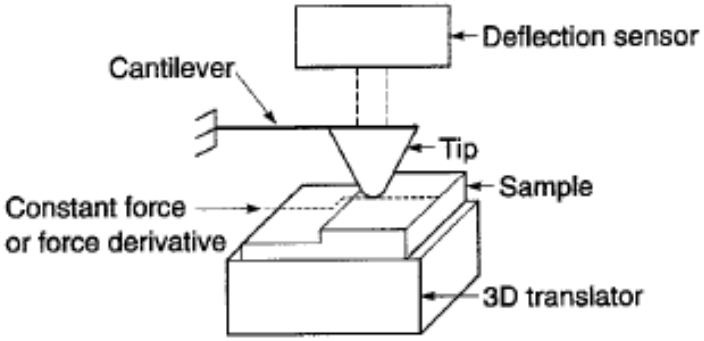

Figure 2.18 Schematic of the key components present in an atomic force microscope. Reproduced from (Bhushan, 2001).

The most popular mode of operation for the deflection sensor is beam deflection method, when the laser light is reflected from the smoothly finished back surface of the cantilever and the deflection of the reflected beam is measured using a photodiode array (which, in simple cases, may consist of just two photodiodes). The beam deflection method can reliably detect cantilever deflection of the order of 10 nanometers -- this number is limited by the thermal noise in the mechanical and the electronic components of the instrument, but may be improved by cooling.

Other deflection measurement techniques include the above mentioned optical interferometry (because the deflections are so small, this requires a very stable laser), piezoelectric detection (for quartz cantilevers or cantilevers made out of other piezoelectric materials), capacitative detection (which relies on the change in capacitance in an electromechanical circuit) and piezoresistive detection (similar to piezoelectric, but resistance is measured).

The primary advantage of AFM over macroscopic cantilever and interferometric methods discussed above is its atomic-scale resolution – it is possible to image individual molecule absorbed at the surface. The AFM technique is therefore uniquely positioned to study complicated surface chemistry processes, such as adsorption and chemical catalysis, as well as assist in creation of atomic-scale patterned media. A disadvantage, however, is the extremely small surface area that may be accessed in a given run of an AFM experiment and, consequently, the impossibility of characterizing macroscopic surface properties, such as the radius of curvature. AFM is therefore not well adapted for macroscopic engineering applications and, at least at the moment, is only used in nano-scale materials engineering – if the curvature of an aspherical lens needs to be confirmed, the interferometry-based methods are still the methods of choice.

2.3.2 Scanning tunneling microscopy

This technique utilizes the quantum phenomenon of *tunneling* – the ability of electrons to cross a potential energy barrier that, according to the laws of classical physics should prevent such a possibility. As with AFM, a tip (usually made of tungsten or platinum-iridium alloy) of very small (nanometers) dimensions is scanned over (but not in contact with) a surface, so that a resulting tunneling current (electron flow from the surface – see Figure 2.19) is passed through the tip and measured. Differences in surface height lead to changes in the current produced and so allows for a very detailed, very high resolution surface profiling (Binnig and Rohrer, 1987). The STM can be operated in two modes: *constant height* where the voltage applied to the tip along with the height of the tip in proximity to the surface are held constant while the current varies and *constant current* where conversely voltage and height are varied in order to maintain a constant charge density at the surface.

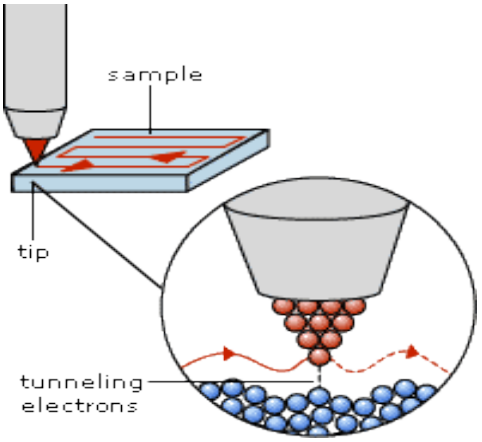

Figure 2.19 Illustration of the basic underlying principle of a scanning tunneling microscope or STM. Reproduced from (Binnig and Rohrer, 1987).

Each mode has certain advantages in terms of operator use and flexibility. Irrespective of the operational mode, the sample must be conductive enough to facilitate a high enough electron flow from the surface through the tip. For a non-conducting sample, this essential requirement may be met by coating the surface with a thin film of conducting material (Bhushan, 2001; Binnig and Rohrer, 1987).

Another important variation of STM is the spin-polarized STM, where a ferromagnetic tip is used that generates spin-polarized electrons that can only be accepted by certain orbitals of the sample (some electronic tunneling transitions are spin-forbidden). The STM method can thus probe the *quantum mechanical structure* of the surface as well as its mechanical and topographical characteristics – the strength of the tunneling current is a function of local electronic as well as mechanical properties. The physical phenomenon in question is called *tunnel magnetoresistance* and the construction that shows this effect is known as *spin valve*. To avoid magnetizing the surface, antiferromagnetic tips are sometimes used in place of the ferromagnetic ones.

Importantly, the STM hardware cannot directly distinguish between the reduction in the tunneling current due to a different quantum mechanical properties of the surface from the reduction that would result from the tip simply moving further away from the surface (both effects are also highly non-linear). It is therefore necessary to use the topographic information

from another source (such as traditional STM or any of the methods described above) and then superimpose the spin-valve STM data on top of that to extract the information pertaining specifically to the magnetic properties of the surface.

Chapter 3

3. Instrument calibration and data processing

Whatever method, instrument or parameters are selected for the measurement of surface profile, the first step to be taken is that of calibration. This process is essential to ensure reliable and reproducible data. If the instrument is in a setting where it is available to any authorized user, calibration is vital as the previous use may have involved a radically different surface sample and choice of instrument parameters, as well as possibly being operated under differing ambient conditions, *i.e.* there is generally instrument sensitivity towards changes in temperature and relative humidity of the surrounding air. For this purpose, a set of carefully stored and maintained calibration standards (samples of known composition and surface details) is made available with the instrument together with a strict printed protocol for the user to follow to ensure a correct calibration step-by-step procedure. Aside from these general considerations, individual methods/instruments may deviate and have their own specific protocols and calibration standards.

3.1 Calibrating stylus-based profilometers

Three main types of standard (example profiles are shown in Figure 3.1) are available for the accurate calibration of a stylus profilometer prior to analysis of the sample of interest:

(1) Depth measurement standard, in which the step height is used for checking vertical magnification factor of an instrument. The standard has wide grooves of known depth.

(2) Spacing measurement standard, which is used for calibrating of the vertical and horizontal profiles. It has a triangular section or repetitive sinusoidal grooves.

(3) Roughness measurement standard, which is used for checking the overall calibration of an instrument. The roughness standard has a pseudo-random profile.

For case (2), the standard profile is chosen for low waviness to ensure easy relocation from place to place, high uniformity (low roughness) and valley dimensions that exceed the size of the stylus tip (so the tip traces the full valley profile). With this type of standard, the instrument

is adjusted in order until the known arithmetic mean roughness parameter (R_a) is measured repeatedly.

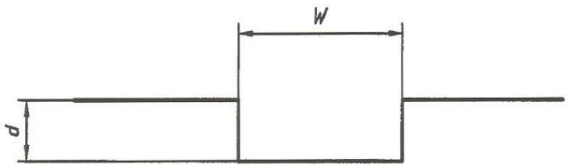

Depth measurement standard

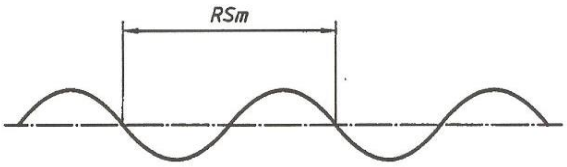

Spacing measurement standard

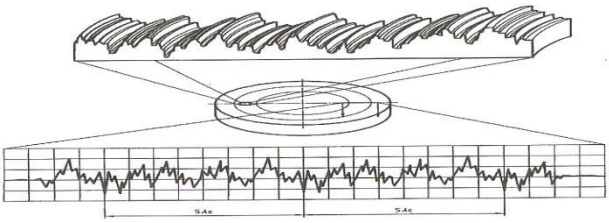

Roughness measurement standard

Figure 3.1 Examples of surface profiles from three types of calibration standard used in stylus profilometers. Reproduced from (ISO25178, 2012).

3.2 Calibrating interferometric profilometers

Because the purpose of this work is to compare the measurement results of stylus-based and interferometry-based instruments, the set of standards used for the interferometric data set was chosen to be the same as that described above for the stylus-based instrument.

Interferometric instruments can scan both lateral dimensions of the sample and therefore, for an interferometric instrument calibration, it is important to calibrate both laterally (in the direction perpendicular to the sample surface) and vertically (in the direction in which the optical scanning is performed during a measurement). Spatial calibration is required to obtain

accurate 2D surface measurement and usually results in the need for some degree of correction factor to be applied before measurement of the sample surface itself. Normally, the calibration standard for this is a specific patterned substrate such as an accurately characterized grid. This process acts to precisely set instrument magnification as determined by the optical configuration and sensor/detector type.

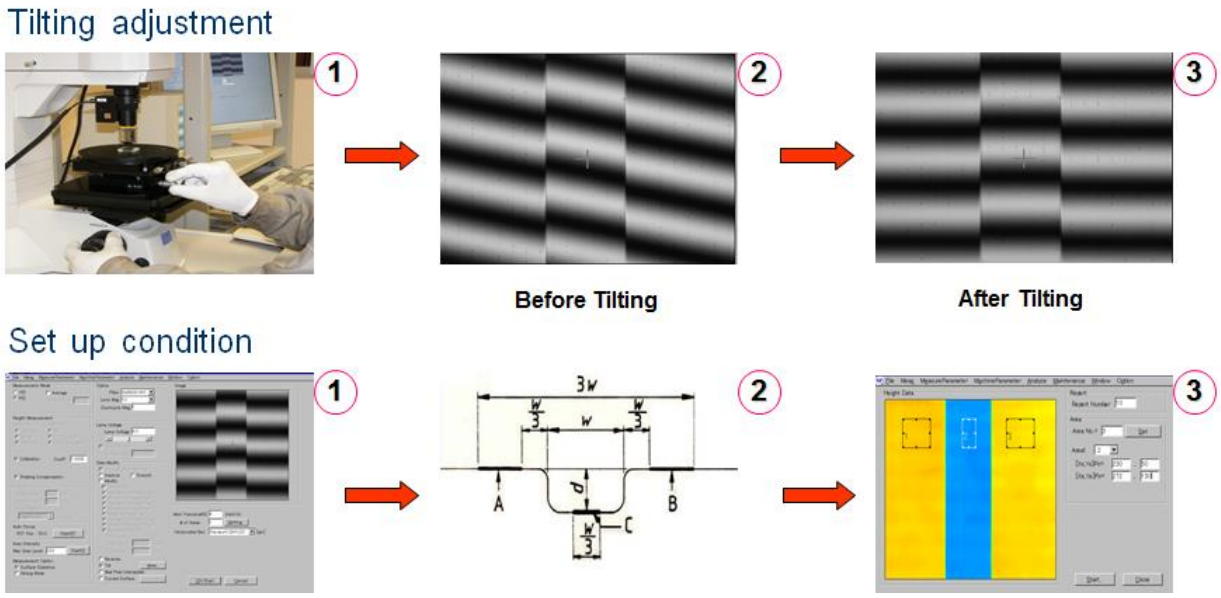

Figure 3.2 Schematic representation of the calibration flowchart for a VSI profilometer.

Vertical calibration corrects for any effects in the *z* direction such as any temporary 'glitches' in gears/motors within the mechanical components of the instrument that can induce undesired motions or non-linearity effects in the vertical dimension. The most common form of calibration standard for this is a step height of very accurately measured dimension that ideally is of a similar order of magnitude to that likely to be present in a sample.

3.3 Data Filtering

The 'raw' data acquired from any technique for surface texture measurement will contain a mixture of, in this case, the desired property of roughness, but also of waviness that results from the manufacturing process – see Figure 3.3 for an illustration of the intertwined nature of these two surface properties. Even for a perfect machining tool that would in theory impart zero waviness on a surface, there will still be some degree of roughness produced.

Consequently to extract a 'pure' roughness signal from a measurement, a subsequent data treatment or *filtering* stage is necessary after the raw data has been obtained (Raja et al., 2002).

The most immediately obvious difference between roughness and waviness is the characteristic length scales on which they occur. Waviness is generally of a significantly longer wavelength than roughness but can be either periodic or non-periodic (as shown in Figure 3.3).

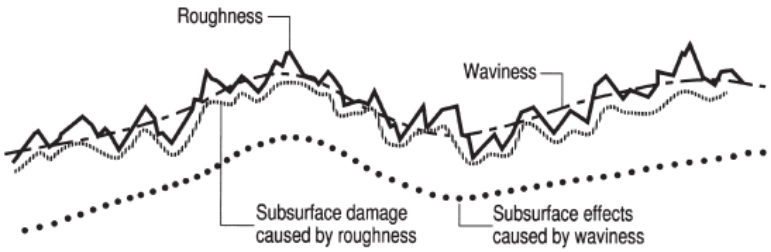

Figure 3.3 Illustration of the inherent 'mixing' of both roughness and waviness from a surface profile. Reproduced from (Whitehouse, 2000).

The most commonly used type of filter for isolating the roughness from a raw surface profile measurement is an electrical network referred to as a 2CR filter as it consists of two capacitor-resistor circuits configured such that the cut-off frequency or wavelength occurs at a transmission value of 75% (Figure 3.4).

The characteristic wavelength at that the 75% transmission occurs is generally known as the filter cut-off or *sampling* length (λ_c). This parameter forms one of three 'length' factors that are key to specify in any measurement of surface texture.

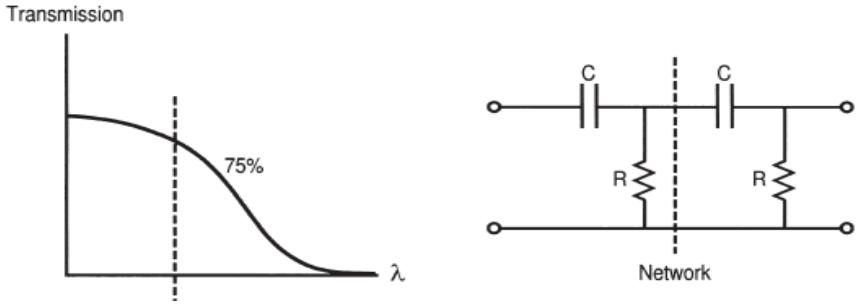

Figure 3.4 Equivalent circuit diagram for the 2CR filter: (left) position of the cut-off wavelength in the transmission profile for a standard 2CR network (right). These are used to isolate a roughness signal from raw data. Image reproduced from (Whitehouse, 2000).

The other two parameters are the *assessment* or *evaluation* length – the scale over that a roughness measurement is made, and the *traverse* length that refers to the distance physically traversed in the course of an individual measurement (see Figure 3.5). The assessment length can be an arbitrarily selected value but conventionally it is set at a value corresponding to $5\lambda_c$. The traverse length is always larger than both sampling and assessment lengths. Typical recommended values for sampling and assessment lengths are shown in Table 3.1 below.

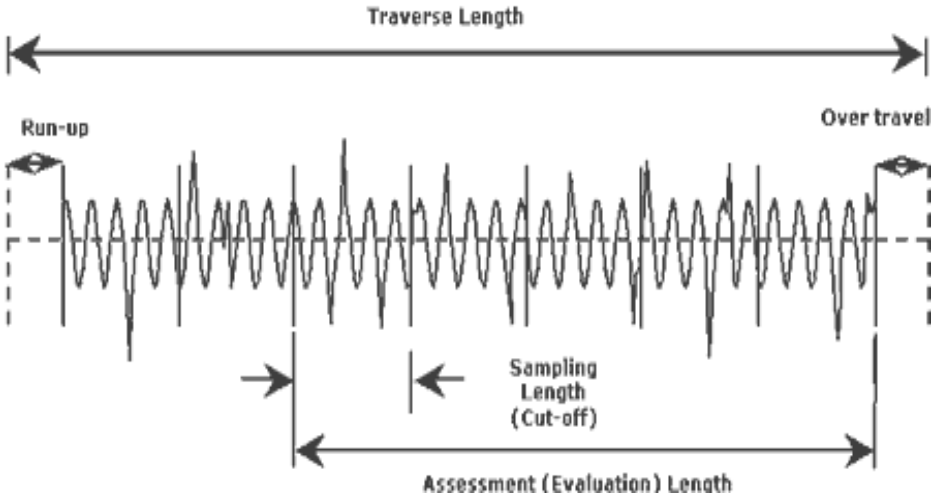

Figure 3.5 Illustration of the characteristic length parameters associated with surface texture measurement. Reproduced from Rapp Industrial Sales web site (http://www.rappindustrialsales.com/).

Table 3.1 Characteristic length dimensions for profile/texture measurements on non-periodic surfaces for R_a ranges as indicated. Reproduced from (Whitehouse, 2000).

R_a / microns	Roughness sampling length / mm	Roughness assessment length / mm
$0.006 < R_a \leq 0.02$	0.08	0.4
$0.02 < R_a \leq 0.1$	0.25	1.25
$0.1 < R_a \leq 2$	0.8	4.0
$2 < R_a \leq 10$	2.5	12.5
$10 < R_a \leq 80$	8.0	40.0

One downside of the 2CR roughness filter is that it imparts a measure of distortion in the signal as a result of a delay in the mean trace of sample waviness relative to the overall profile (containing the roughness detail). This overestimates the true values of some of the characteristic amplitude parameters, but in the case of the arithmetic average (R_a), the error is

minor (1-2%). If those parameters that are more significantly distorted are those required from measurement, then alternative, more recently developed filter types (*e.g.* a phase-corrected form, such as the Gaussian filter, for which λ_c occurs at 50% signal transmission) are available.

3.4 Environmental considerations

A stable environment (temperature, humidity, vibration, *etc.*) is essential for achieving reliable measurements that are accurate and reproducible. CSI is based on light interferometry and the detection of light fringes – fringe stability is easily affected by vibration, air turbulence and temperature. The same applies to stylus instruments that are also easily perturbed by these factors.

Vibration influences the stability of the VSI fringe patterns and the position of the stylus. Isolation systems may be used to reduce the vibration caused by street traffic or nearby equipment, but care must be taken to ensure that the isolation system is capable of damping the required frequency range. Acoustic noise can also generate vibrations, and it is therefore a good idea to position the profilometric instrument far from external noise sources.

Another important factor is air turbulence – air flow between the sample and objective lens can generate small phase errors and perturbations in the light fringes due to the instantaneous changes in the refractive index of the air. Airflow can also be a source of vibration. For this reason, care should be taken to prevent currents from passing through the instrument by positioning it far from *e.g.* the air conditioning systems. More generally the changes in the atmospheric air pressure are harder to control – the corresponding effects must be recorded and taken in to account during instrument calibration. Modern VSI instruments have internal compensation mechanisms for those effects, in which case it is necessary to enter the corresponding environmental parameters into the instrument calibration system.

The third critical factor is temperature stability. It is particularly important for the geometric stability of the instrument frame – the instrument must be located in a thermally stable room and far from any sources of temperature perturbation or air currents. If the ambient temperature in the room is expected to change, care must be taken to ensure that the change

is minimal and occurs in well-defined time periods. For this reason, it is a good idea to place all profilometric instruments away from direct sunlight.

The final factor is the general cleanliness of the instrument environment – one must ensure that the air circulating in the room does not contain any particles or aerosols. High-precision measurements are best performed in a clean room.

Chapter 4

4. Measurement protocols

This chapter provides a detailed description of the materials and methods used in the present work, including the detailed experimental protocols that will be of use to the future generations of researchers working on a similar topic. It follows on to the results and discussion section, where the data is presented, analyzed, and the conclusions are drawn about the relative merits of the two methods and about the possibility of combining their data into a single dataset that would be more resilient to method-specific distortions.

The sample surfaces chosen for study were of a standard made from quartz glass with nominal value of step height (0.330 and 2.340 µm) and tungsten metal with roughness parameter R_a and R_z values of 0.400 and 1.500 µm respectively (ISO5436, 2000). Measurements were made with both a stylus profilometer and VSI instrument for comparison of accuracy and repeatability of data. Specifications and measurement protocols for both instruments are now detailed.

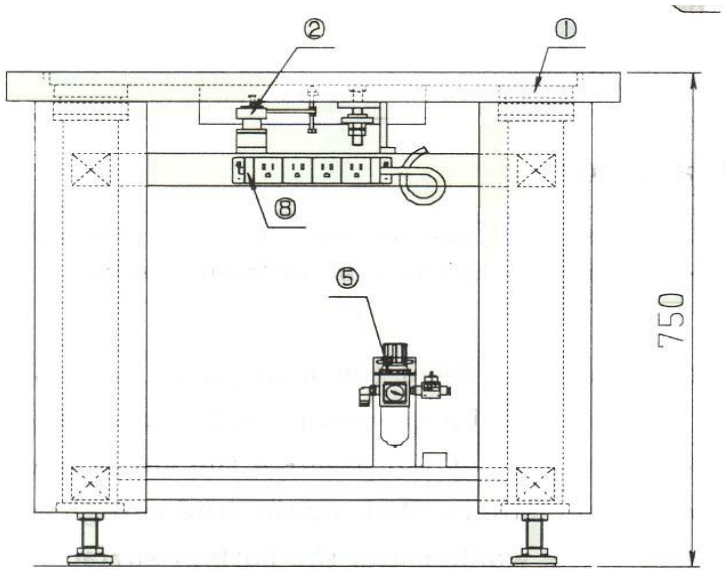

Figure 4.1 Schematic diagram of the pneumatic vibration isolation table system. The pressure gauge is located in the top right corner of the table.

All measurements reported in this experiment were performed on vibration isolation systems (Figure 4.1) – it is absolutely essential that environmental vibrations are dampened because their frequencies overlap significantly with the mechanical frequencies of the measurement systems.

4.1 Step height and roughness standards

The roughness standards used in this work are shown in Figure 4.2 below.

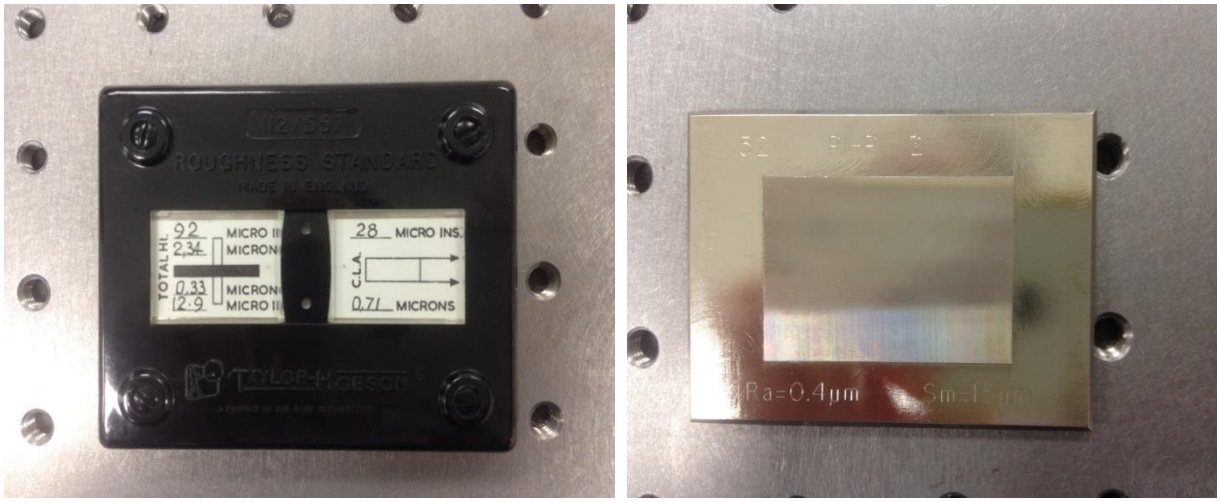

Figure 4.2 Surface standards used in this work: (left) step height standard and (right) roughness standard.

The step height and roughness standard (as shown in the figure 4.2) have to be cleaned before the measurement begins by the standard cleaning procedure. The following cleaning procedure was applied:

1. Clean the step height and roughness standard using ethyl alcohol and wipe off with soft lint-free cloth or appropriate wiper.

Figure 4.3 Cleaning process (wiping – left and blow drying – right).

2. Stabilize the step height standard for at least 1 hour before measurement.

The stabilization process is necessary because the geometric parameters of the standard, as well as of the measurement instrument, depend on temperature and, to a lesser extent, atmospheric pressure (Hariharan, 2003, Whitehouse, 1997). For this reason, calibration samples should be stored near the instrument in an environment that has been stabilized with respect to temperature and humidity.

4.2 Stylus instrument: initial setup

Below is a step-by-step protocol that was followed for the preparation and operation of the stylus-based instrument, including screen shots from the related software packages. Brief comments are also included on the purpose of each of the procedures performed. Stylus instrument specifications are as follows:

- Model: *Kosaka Laboratory ET4000AK*
- X-axis – measuring range of 100 mm, resolution of 0.01 µm
- Z-axis – setting range of 52 mm, LVDT transducer, measuring range of 32 µm, resolution of 1 nm, tip force range of 0.5-500 µN, tip radius of 2 µm
- Ambient temperature measured by digital thermometer at 20 ± 1 ºC / relative humidity at 50 ± 10%.

The start-up sequence is as follows:

1. Turn on the pneumatic vibration isolation system. This ensures that the system is adequately insulted from the mechanical noise present in its environment.
2. Check the air pressure from the pressure gauge under the pneumatic vibration table. Ensure that, the pressure gauge is between 0.45 MPa and 0.55 MPa (Figure 4.4). This ensures that the table floats at its optimum height.
3. Turn the power on to remote control unit, amplifying operation unit, CCD unit, main unit and personal computer in roughness measuring instrument (see the schematic diagram above) and leave it to be stabilized for least 30 minutes. The stabilization period is necessary because the electrical characteristics of the electronics are temperature-dependent and the temperature distribution takes time to reach the equilibrium state after the system is powered on.

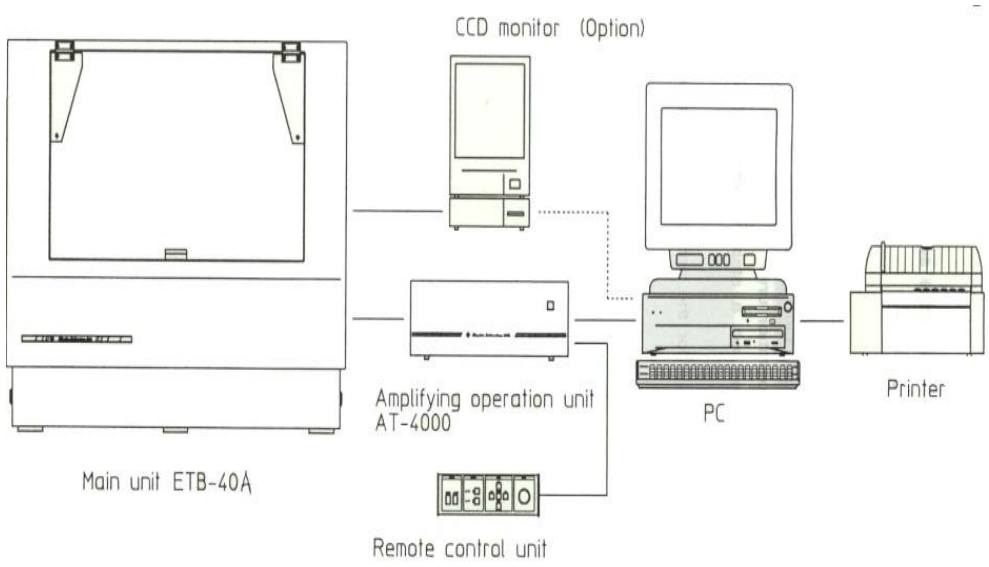

Figure 4.4 Schematic diagram of the stylus instrument.

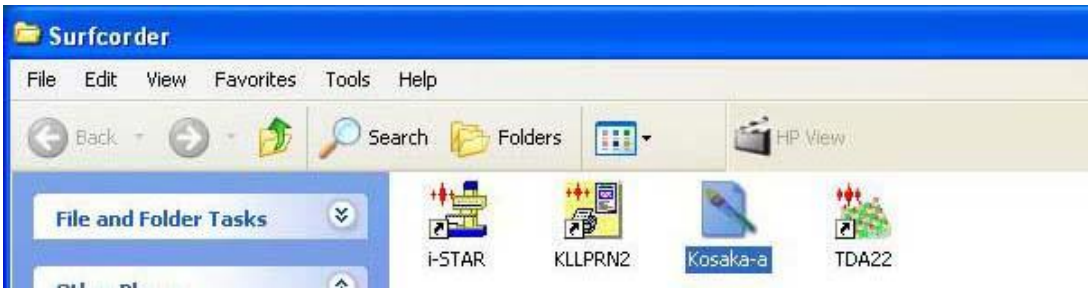

Figure 4.5 Screenshot of the Windows Program Manager folder containing the stylus software start-up icons.

4. Double click i-STAR icon in the Surfcorder folder (see the screenshot above). After that, the screen displays “Start the initialization” box. Select OK in “Start the initialization” box. After that, the instrument will initialize along X and Y axes.
5. After that, screen displays “Initialize the pick-up”. Select "Pick-up init" in the initialization box. The instrument will initialize along the Z axis. After that, the screen display “Initialization finished”. Press the "close" button. The screen will launch into I-Star program.

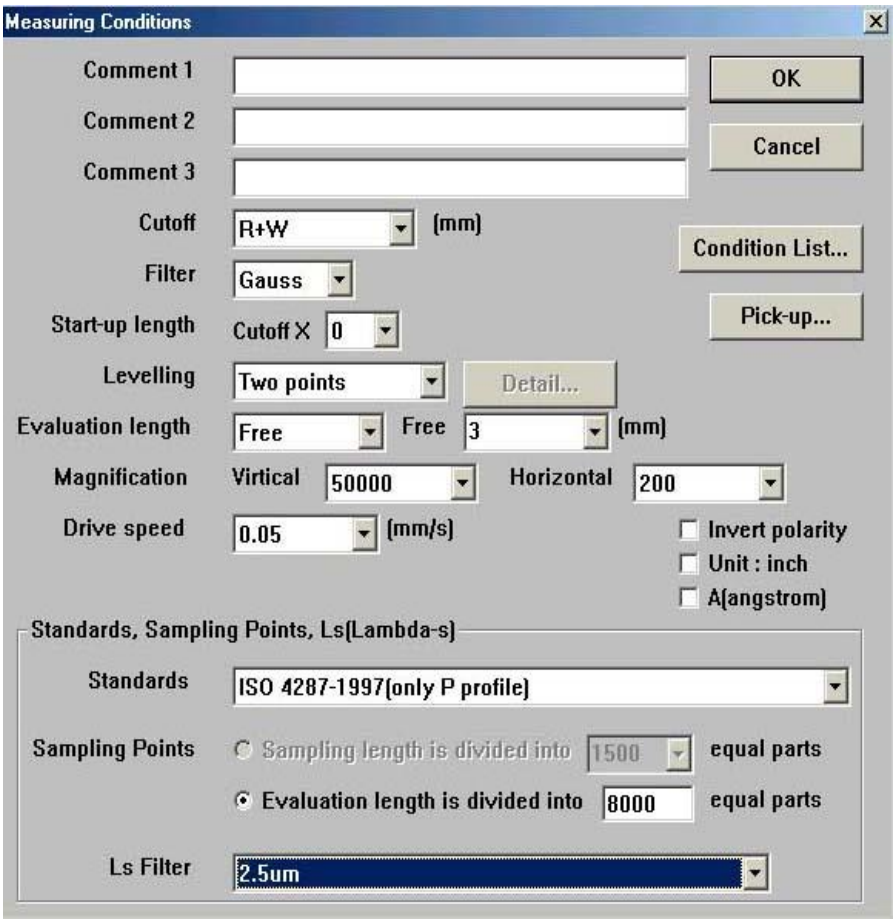

Figure 4.6 Parameter selection window of the stylus profilometer control software.

The parameter selection window of the measurement process is largely self-explanatory – the parameters in question have been described in the introduction chapters above.

4.3 Stylus instrument: step height measurement

The step height measurement sequence on the stylus instrument is as follows:

1. Put the step height standard on middle position of instrument table.
2. Move Z axis until close to surface of the step height standard using remote control unit.
3. Press “AUTO” button on remote control unit. The pick-up unit will move automatically to the surface of the step height standard until the stylus moves to middle measurement range.
4. Assign the measuring area. Number of traces must be not less than five and shall be distributed over the measuring area (refer to ISO 5436-1:2000).

5. Align the measurement area in X and Y axis by remote control unit and adjusting the step height standard by hand and the traversing direction should be perpendicular to the direction of the lay unless otherwise indicated.
6. Tilt the measurement plane of the step height standard using 'Tilt' adjusts command in Control menu of *I-Star* program.
7. Select X auto adjust button on "Tilt adjust window". The X-tilt Auto Adjust will display. Insert the tilting length into the windows. Note: Tilting length must be cover the measurement length of the step height standard
8. Select 'Done' button on X-tilt Auto Adjust window. The instrument will tilt the measurement plane of the step height standard. Then select 'Close' button on X-tilt Auto Adjust window.
9. Select 'Measuring Conditions' menu and set using following criteria;

    Standards: ISO 4287-1997 (Only P profile).

    Cutoff: R + W.

    Filter: Gaussian.

    Evaluation length: depends on the width of groove of the step height standard.

    Magnification Vertical: 20000 / Horizontal: 200.

    Drive speed: 0.02 mm/s.

    Sampling points: 8000 points.

10. Select "Measure toolbar". The instrument will automatically start measurement. The number of repeat measurements n = 5.
11. After finishing, select "Save toolbar" for saving measurement data.
12. Move the step height standard to next line and repeat previous step until all measurements are complete.
13. Save the results of measurement to ASCII text file format for subsequent analysis in a spreadsheet program.
14. After finishing measurement, move the stylus from the step height standard and remove the step height standard from the table.

4.4 Stylus instrument: roughness measurement

The roughness measurement sequence on the stylus instrument is as follows:

1. Put the roughness standard in the middle position of instrument table.
2. Move Z axis by remote control unit until close to surface of the roughness standard.
3. Press “AUTO” button on remote control unit. The pick-up unit will move automatically to the surface of the roughness standard until the stylus moves to the middle of the measurement range.
4. Assign the measuring area. Number of traces must not be less than twelve and should be distributed over the measuring area.
5. Align the measurement area in X and Y axes by remote control unit and adjusting the roughness standard by hand. The traversing direction should be perpendicular to the direction of the lay unless otherwise indicated.
6. Tilt the measurement plane of the roughness standard using Tilt adjusts command in Control menu of I-Star program.
7. Select X auto adjust button on Tilt adjust window. The X-tilt Auto Adjust will display. Insert the tilting length into the windows. Note: Tilting length must cover the measurement length of the roughness standard.
8. Select “Done” button on X-tilt Auto Adjust window. The instrument will tilt the measurement plane of the roughness standard. After finishing, select Close button on X-tilt Auto Adjust window.
9. Select Measuring Conditions menu and set measuring conditions as follows;.

    Standards: ISO 4287:1997 (Roughness).

    Cutoff: refer to ISO 4288:1996

    Roughness sampling length: 0.8mm.

    Filter: Gaussian.

    Evaluation length: Refer to ISO 4288:1996, roughness evaluation length 4.0 mm.

    Magnification Vertical: 20000, Horizontal: 200.

    Drive speed: 0.02 mm/s.

    Sampling points: 8000 points.

10. Select Measure toolbar. The instrument will automatically start measurement. The number of repeat measurements n = 5.
11. After finishing, select “Save” toolbar for saving measurement data.
12. Move the roughness standard to next line and repeat until complete measurement.
13. After finishing, following operation;
14. Move the stylus from the roughness standard
15. Remove the roughness standard from the table

A schematic diagram of the layout of the step height and roughness standard sample used in this work is given in Figure 4.7 below.

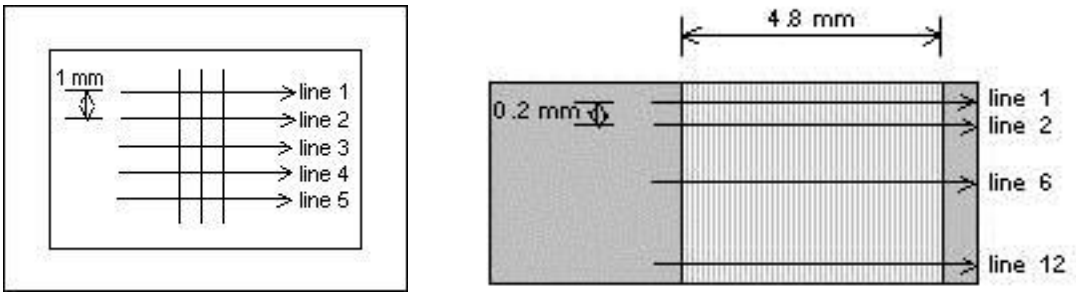

Figure 4.7 Measurement areas for the Taylor Hobson step height and roughness standard.

4.5 VSI instrument: initial setup

The VSI instrument is considerably more sophisticated. In particular, there is no restriction on sample surface – the surface does not have to be smooth with the height range within several micrometers, and even rough surfaces can be measured. Below is a step-by step protocol for the preparation and operation of the VSI instrument, including screen shots from the related software packages. Brief comments are also included on the purpose of each of the procedures performed. VSI instrument specifications are as follows:

- Light source: 100 W halogen lamp (Osram Phillips) – wavelength resolution of 1 nm.
- Objective lens: Nikon WD 9.3 - 5x (Field of view size: 0.77 mm x 0.72 mm).
- Microscope: Nikon Eclipse L150 (see *Appendix E*)
- CCD: Sony EO-3112 (480 x 512 pixels)
- Ambient temperature measured by digital thermometer at 20 ± 1 ºC / relative humidity at 50 ± 10%.

The start-up sequence is as follows:

1. Turn on the pneumatic vibration isolation system. This ensures that the system is adequately insulted from the mechanical noise present in its environment.
2. Check the air pressure from the pressure gauge under the pneumatic vibration table. Ensure that, the pressure gauge is between 0.45 MPa and 0.55 MPa (Figure 4.1). This ensures that the table floats at its optimum height.
3. Turn on the power supply of the instrument.
4. Turn on the personal computer.

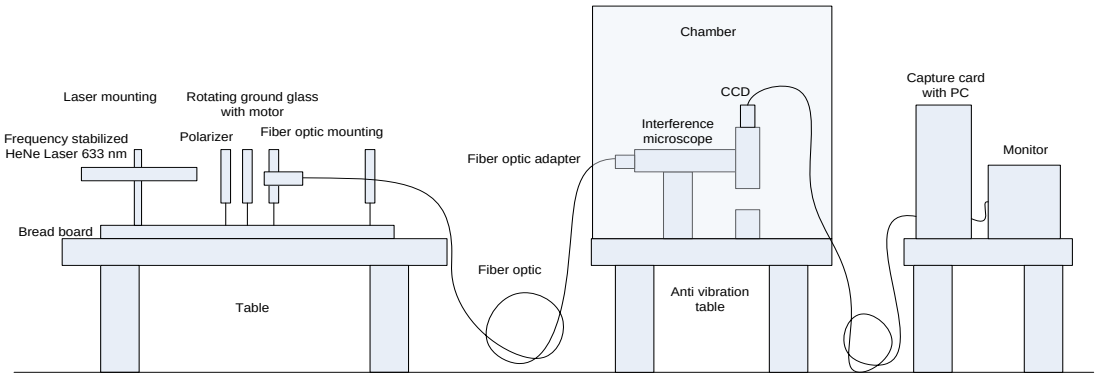

Figure 4.8 Step height standard measuring instrument system.

5. Double click SP-500 icon on the desktop. After that, the screen display SP-500 window, then click **[OK]** with no password entered.
6. Click **[Load Parameters As]** from [File] menu. Select the VSI parameter from the **Parameters** folder.
7. Click **[Measure Parameter]** menu. Detail of the parameters selected in step 6 can be checked and modified there (see in Figure 4.9).
8. Left the instrument system at least 30 minutes for them to be stabilized.

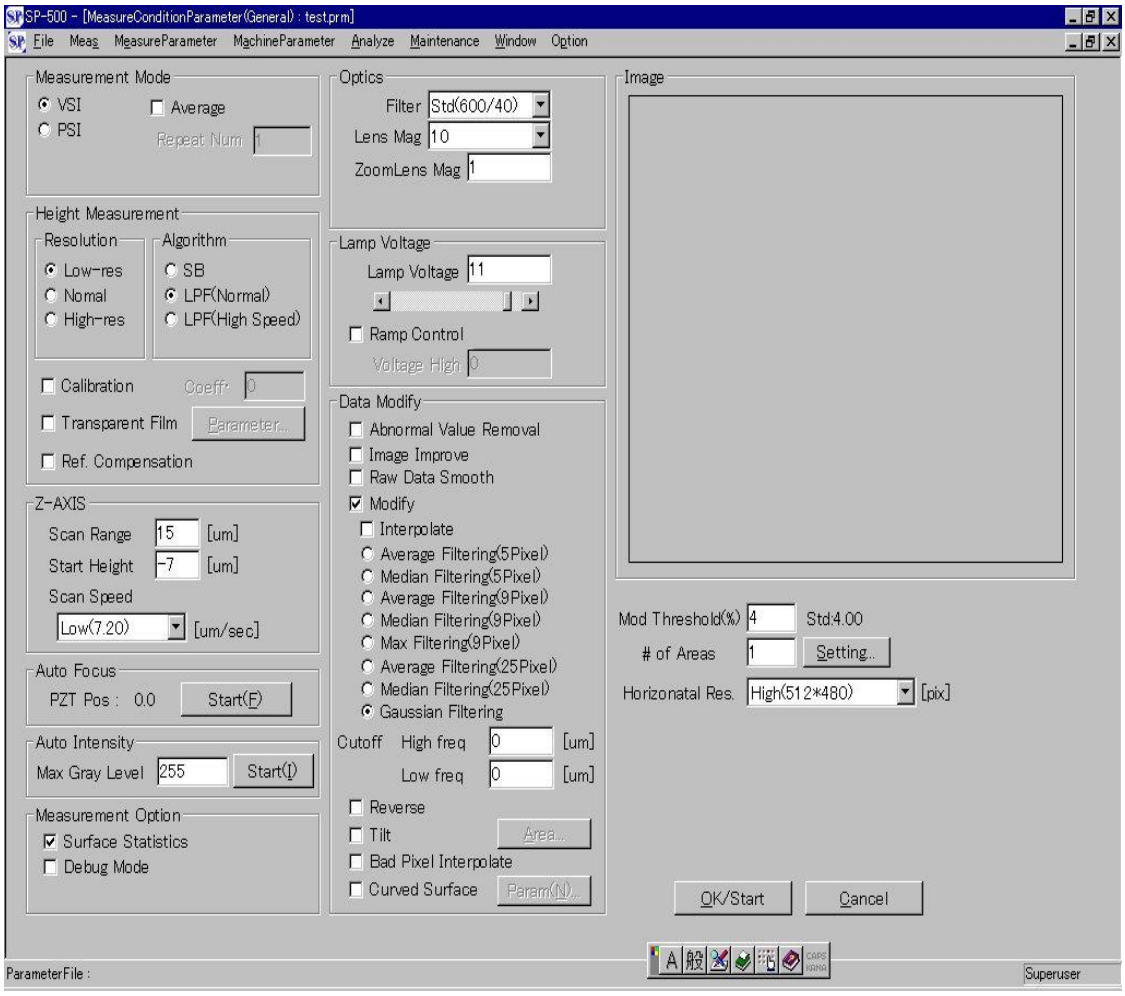

Figure 4.9 Measurement conditions window.

4.6 VSI instrument: step height measurement

For step height measurement it is very important to adjust the position of the sample surface so that the surface is perpendicular to the optical axis. This process is called levelling and VSI instruments usually have some form of tip and tilt adjustment, either manual or automatic. Tip and tilt adjustment can be monitored in real time on the instrument screen by looking at the white light fringe pattern. A poorly levelled sample would have a large number of closely spaced fringes. As the sample levels into the correct position, the fringe spacing would increases until the null fringe condition is reached – it looks like one large fringe that blink on and off as the instrument scans the vertical axis. The null fringe condition may be hard or impossible to achieve if the surface has slowly varying features.

The step height measurement sequence on the VSI instrument is as follows:

1. Put the step height standard on the stage.
2. Rotate the height adjustment knob of the stage and raise the stage along the Z axis until an interference fringes pattern appears on the monitor.
3. Make a tilting adjustment of the stage for leveling the step height standard surface. The tilting adjustment must be performed until there is no fringe on the screen but the step height standard is still in focus.
4. Adjust **[Lamp Voltage]** to make the image in the **Measure Condition** display slightly red. Then decrease the voltage until red dots disappear completely.
5. Select **[Measurement Mode]**, click selects **[VSI Mode]**.
6. Check the measuring conditions in the **Measure Condition** window that the VSI mode is selected.
7. Z-axis: The scan range must be at least 2 times of the height of the step height standard. The start point will be automatically adjusted to half of the scan range.
8. Click **[OK/Start]** to start measurement.
9. Click **[Save Height Data As]** in **[File]** menu to save the measurement result.
10. Repeat step 4 more times.
11. Assign the measurement area, number of area measurement around five and should be distributed over the measuring surface area

When interpreting step height measurements using VSI technique, care must be taken to account for the interferometric artefacts described above – the present work assumed that those artefacts are negligible, but their presence is a distinct possibility that should be investigated in the future work. One possible indicator would be the presence or absence of sinusoidal fringes around the step in the computer reconstruction.

4.7 VSI instrument: roughness measurement

A critical parameter for VSI roughness measurement that can significantly influence the outcome, if incorrectly set, is the lamp voltage, or equivalently, the light intensity. Because the height measurement in VSI is phase-based and the saturated areas on the detector carry no

phase information, the picture may become "drowned" with saturated areas. When that happens, deeper parts of the image effectively rise and the roughness measure, which essentially relies on the difference between the highest and the deepest parts of the sample, is incorrectly computed. For this reason, the light intensity must be adjusted to prevent saturation. The saturated areas are colored red in our instrument – there should be no red spots left when the lamp voltage is adjusted.

The roughness measurement sequence on the VSI instrument is as follows:

1. Put the roughness standard on the stage.
2. Rotate the height adjustment knob of the stage and raise the stage along the Z axis until an interference fringes pattern appears on the monitor.
3. Make a tilting adjustment of the stage for leveling the roughness standard surface. The tilting adjustment must be performed until there is no fringe on the screen but the roughness standard is still in focus.
4. Adjust **[Lamp Voltage]** to make the image in the **Measure Condition** display slightly red. Then decrease the voltage until red dots disappear completely.
5. Select **[Measurement Mode]**, clicks select **[VSI Mode]**.
6. Check the measuring conditions in the **Measure Condition** window that the VSI mode is selected.
7. Z-axis: The scan range must be at least 2 times of the height of the roughness standard. The start point will be automatically adjusted to half of the scan range.
8. Click **[OK/Start]** to start measurement.
9. Click **[Save Height Data As]** in **[File]** menu to save the measurement result.
10. Repeat step 4 more times.
11. Assign the measurement area, number of area measurement around five, ten and twenty position and should be distributed over the measuring surface area

An important matter for the processing and interpretation of VSI roughness that this thesis is too small for but that needs careful analysis is the impact of the digital filtering on the resulting value of the roughness parameter. The definition of peak to valley height provided in the

introduction section of this thesis critically relies on the maximum and the minimum surface heights within the area being sampled correctly. However, a notable feature of noise-eliminating convolution filters (Gaussian, low pass, *etc.*) is their *smoothing* effect on the surface. Those filters do serve their purpose of eliminating digitization noise, but they could also in principle adversely affect the measurement outcomes. It would therefore be useful, in future work, to either assess the impact of digital filtering on the resulting roughness values, or to develop a definition of surface roughness that is invariant under the commonly used digital filters.

Chapter 5

5. Results and discussion

This section contains the raw measurement data with descriptive statistics applied, as well as the analysis of the measurement outcomes in terms of accuracy relative to the nominal values and statistical distributions around the apparent mean. The nominal values of the two step height standards are 0.330 µm and 2.340 µm. The nominal values for the roughness standard are R_a is 0.400 µm and R_z is 1.500 µm.

5.1 Step height measurement: stylus method

To gather sufficient statistics for the step height measurement using the stylus method, 25 independent measurements were taken: five standard sample lines with five repeated steps measured for each line. The raw experimental data, along with the descriptive statistics, is presented in Table 5.1 below.

Table 5.1 Measured step height data for 0.330 µm and 2.340 µm standards using the stylus method.

Measurement position (scan number)	Step height :0.330 µm (µm)	Step height :2.340 µm (µm)
Line 1		
1	0.324	2.326
2	0.324	2.326
3	0.324	2.327
4	0.323	2.326
5	0.323	2.363
Line 2		
1	0.321	2.321
2	0.322	2.322
3	0.322	2.322
4	0.322	2.322
5	0.321	2.321
Line 3		
1	0.320	2.321
2	0.320	2.322
3	0.320	2.321
4	0.320	2.321
5	0.320	2.321

Line 4		
1	0.320	2.321
2	0.319	2.323
3	0.320	2.322
4	0.319	2.322
5	0.319	2.322
Line 5		
1	0.320	2.325
2	0.320	2.325
3	0.320	2.325
4	0.320	2.325
5	0.320	2.325
Mean	**0.321**	**2.325**
Standard deviation	**0.002**	**0.008**

It is likely that the first set of step height standard measurements contain a systematic error since the mean is about five standard deviations away from the calibrated value. The second standard is statistically sound and the mean is within the statistically acceptable distance from the calibrated value. This highlights the possibility that a non-linear calibration may in some cases be necessary: the instrument clearly performs as intended for the second standard, but its calibration appears to be a function of the step size that is being measured. For high-precision measurement this drift should be accounted for, perhaps by making calibration function quadratic, rather than linear.

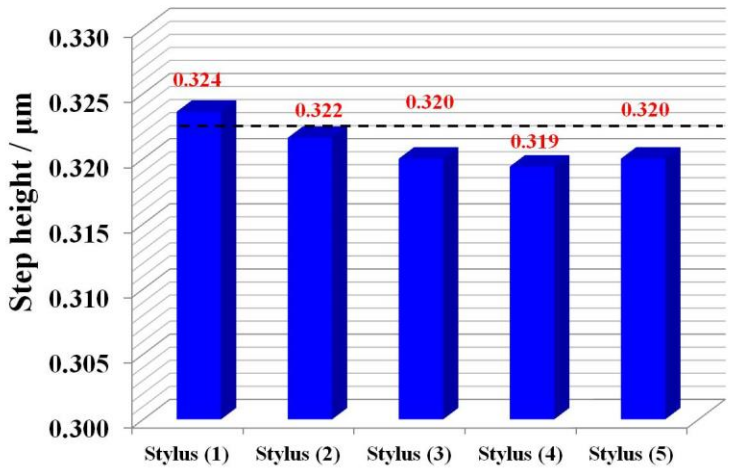

Figure 5.1(a) Mean step height measurements (values in red – from Table 5.1 data) at each of five positions using the stylus profilometer. The dashed line is the average value (0.321 µm) calculated from all positions.

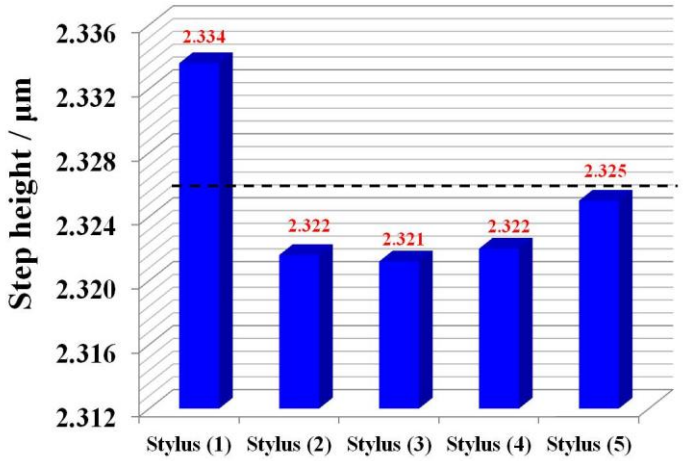

Figure 5.1(b) Mean step height measurements (values in red – from Table 5.1 data) at each of five positions using the stylus profilometer. The dashed line is the average value (2.325 µm) calculated from all positions.

A visual representation of the same data is given in Figure 5.1. The results from both figures have appeared to present a systematic drift. This problem can be caused by the measurement environment, for example temperature. When the temperature in the laboratory is not properly controlled, this type of measurement error could happen.

5.2 Step height measurement: VSI method

To gather sufficient statistics for the step height measurement using the VSI method, 25 independent measurements were taken: five standard sample lines with five repeated measured for each line.

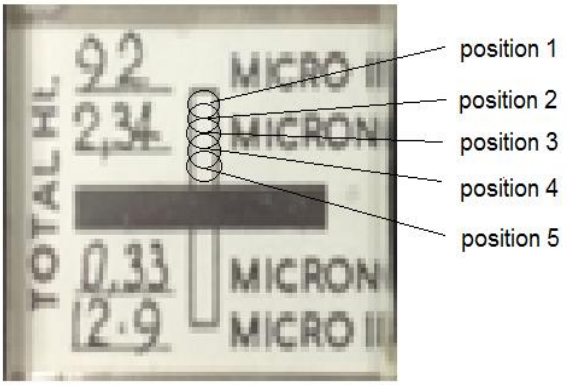

Figure 5.2 The area of step height standard used for the five-position measurement using VSI.

The raw experimental data, along with the descriptive statistics, is presented in Table 5.2 below.

Table 5.2 Measured step height data for 0.330 µm and 2.340 µm standards using the VSI method.

Measurement position (scan number)	Step height (µm)	Step height (µm)
Position 1		
1	0.357	2.427
2	0.352	2.361
3	0.354	2.439
4	0.354	2.405
5	0.354	2.314
Position 2		
1	0.359	2.289
2	0.370	2.657
3	0.371	2.467
4	0.367	2.585
5	0.369	2.492
Position 3		
1	0.393	2.492
2	0.391	2.496
3	0.391	2.456
4	0.391	2.560
5	0.391	2.466
Position 4		
1	0.356	2.336
2	0.356	2.341
3	0.356	2.309
4	0.355	2.318
5	0.356	2.291
Position 5		
1	0.362	2.307
2	0.361	2.384
3	0.359	2.388
4	0.361	2.376
5	0.360	2.400
Mean	**0.366**	**2.414**
Standard deviation	**0.014**	**0.097**

It indicates that the first set of step height standard measurements shows the error +0.074 µm with the random error (SD) about 0.014 µm, whilst the second standard shows the error +0.074 µm with the random error (SD) about 0.097 µm. A visual representation of the same data is given in Figure 5.3(a) and (b).

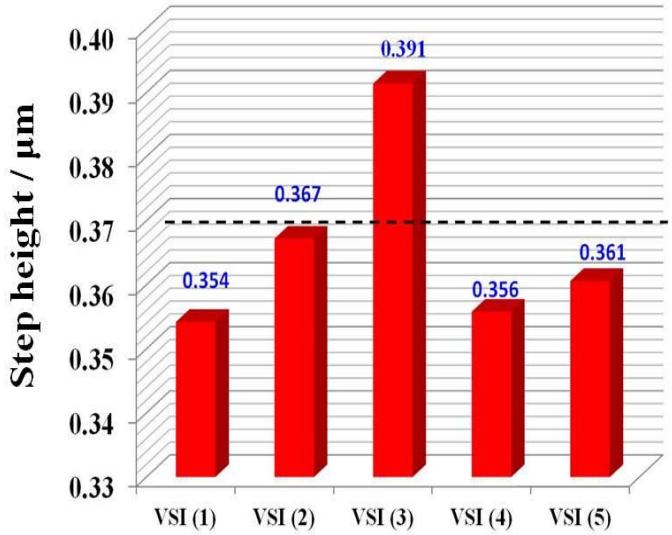

Figure 5.3(a) Mean step height measurements (values in blue – from Table 5.2 data) at each of five positions using the VSI instrument. The dashed line is the average value (0.366 µm) calculated from all positions.

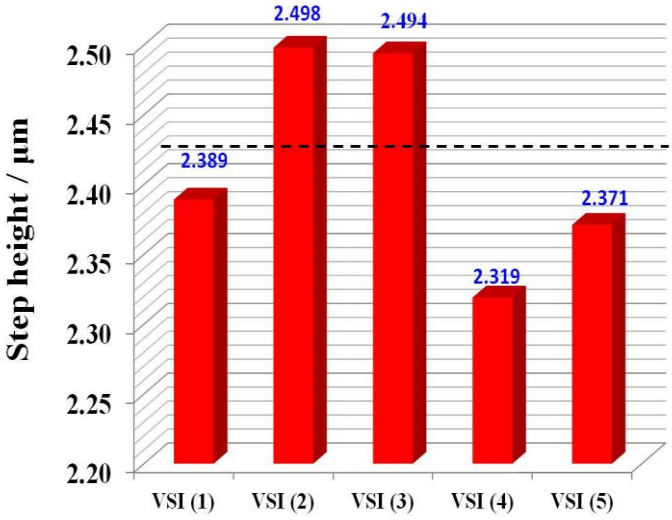

Figure 5.3(b) Mean step height measurements (values in blue – from Table 5.2 data) at each of five positions using the VSI instrument. The dashed line is the average value (2.414 µm) calculated from all positions.

The most obvious observation for the VSI method, as compared to the stylus method, is the much larger standard deviation by a factor of five for both standard samples. The second observation is that the smaller step height sample result is also featuring a statistically significant random error.

A visual representation of the same data is given in Figure 5.3. In this case there appears to be no systematic drift in the measurement value, suggesting that the scatter observed in the data from the VSI instrument is genuinely statistical and is not a consequence of systematic action of any external factors. Still, the much bigger statistical error relative to a mechanical instrument is rather unusual in physical sciences – it has been the case for decades that optical instruments tend to yield superior accuracy to mechanical instruments. It is clearly not the case here. Because in my experiment the measurement result obtained from the stylus instrument has much lower standard deviation than the optical instrument.

5.3 Roughness measurement: stylus method

To gather sufficient statistics for the roughness measurement using the stylus method, 60 independent measurements were taken: 12 sample lines with five repeated measured for each line. The raw experimental data, along with the descriptive statistics, are presented in Table 5.3 below.

Table 5.3 Measured roughness values for the standard with R_a = 0.400 µm, R_z = 1.500 µm using the stylus method.

Measurement position (scan number)	Arithmetic mean R_a (µm)	Max. peak to valley R_z (µm)
Line 1		
1	0.380	1.445
2	0.385	1.450
3	0.387	1.454
4	0.388	1.461
5	0.389	1.465
Line 2		
1	0.377	1.428
2	0.383	1.442
3	0.385	1.448
4	0.386	1.454
5	0.386	1.458

Line 3		
1	0.381	1.439
2	0.384	1.444
3	0.386	1.449
4	0.387	1.450
5	0.387	1.450
Line 4		
1	0.383	1.468
2	0.386	1.470
3	0.387	1.468
4	0.388	1.472
5	0.389	1.473
Line 5		
1	0.380	1.444
2	0.384	1.453
3	0.386	1.458
4	0.388	1.460
5	0.388	1.463
Line 6		
1	0.377	1.423
2	0.382	1.432
3	0.384	1.438
4	0.385	1.440
5	0.386	1.442
Line 7		
1	0.381	1.442
2	0.384	1.443
3	0.385	1.447
4	0.386	1.449
5	0.386	1.451
Line 8		
1	0.385	1.448
2	0.387	1.445
3	0.388	1.448
4	0.389	1.450
5	0.389	1.450
Line 9		
1	0.376	1.451
2	0.384	1.457
3	0.387	1.460
4	0.388	1.462
5	0.389	1.462

Line 10		
1	0.376	1.460
2	0.382	1.462
3	0.385	1.463
4	0.386	1.475
5	0.387	1.462
Line 11		
1	0.378	1.418
2	0.382	1.423
3	0.384	1.429
4	0.384	1.433
5	0.385	1.435
Line 12		
1	0.376	1.426
2	0.382	1.432
3	0.385	1.436
4	0.387	1.440
5	0.387	1.442
Mean	**0.385**	**1.449**
Standard deviation	0.0035	0.013

It has been suggested that the roughness standard shows the error -0.015 µm with the random error (SD) about 0.0035 µm for R_a parameter, whilst the R_z parameter shows the error -0.051 µm with the random error (SD) about 0.013 µm. A visual representation of the same data is given in Figure 5.4 (a) and (b).

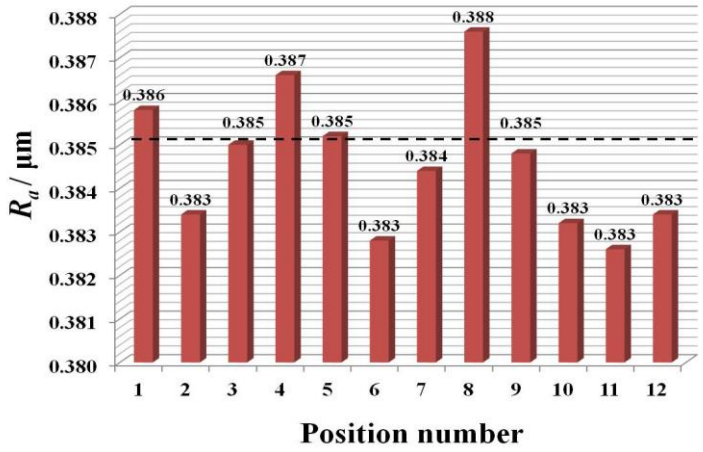

Figure 5.4(a) Mean R_a measurements (from Table 5.3 data) at each of twelve positions using the stylus profilometer. The dashed line is the average value (0.385 µm) calculated from all positions.

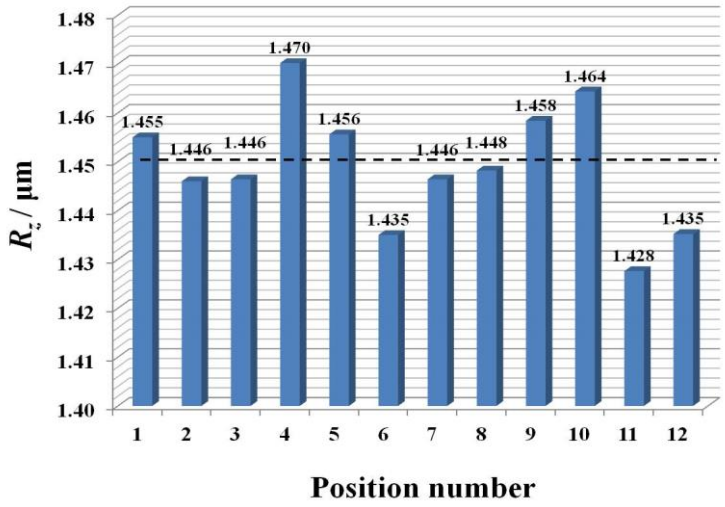

Figure 5.4(b) Mean R_z measurements (from Table 5.3 data) at each of twelve positions using the stylus instrument. The dashed line is the average value (1.449 µm) calculated from all positions.

5.4 Roughness measurement: VSI method

To gather sufficient statistics for the roughness measurement using the VSI method, 25 independent measurements were taken: five sample positions with five repeated measured for each line. The raw experimental data, along with the descriptive statistics, are presented in Table 5.4 below.

Table 5.4 Measured roughness values for the standard with R_a = 0.400 µm, R_z = 1.500 µm using the VSI method. A five-position data set.

Measurement position (scan number)	Arithmetic Mean R_a (µm)	Max. peak to valley R_z (µm)
Position 1		
1	0.392	1.998
2	0.387	1.876
3	0.391	1.955
4	0.393	1.998
5	0.400	1.931
Position 2		
1	0.404	2.375
2	0.402	2.370
3	0.401	2.342
4	0.406	2.402
5	0.398	2.360

Position 3		
1	0.395	1.952
2	0.397	1.988
3	0.396	1.969
4	0.396	1.954
5	0.397	1.985
Position 4		
1	0.371	1.985
2	0.369	1.919
3	0.369	1.903
4	0.369	1.927
5	0.367	2.000
Position 5		
1	0.384	1.919
2	0.382	1.908
3	0.388	1.943
4	0.389	1.979
5	0.388	1.955
Mean	**0.389**	**2.036**
Standard deviation	0.012	0.174

It has been shown that the R_a measurement of the roughness standard shows the error -0.009 µm with the random error (SD) about 0.002 µm, whilst the R_z measurement shows the error -0.015 µm with the random error (SD) about 0.008 µm. A visual representation of the same data is given in Figure 5.5 (a) and (b).

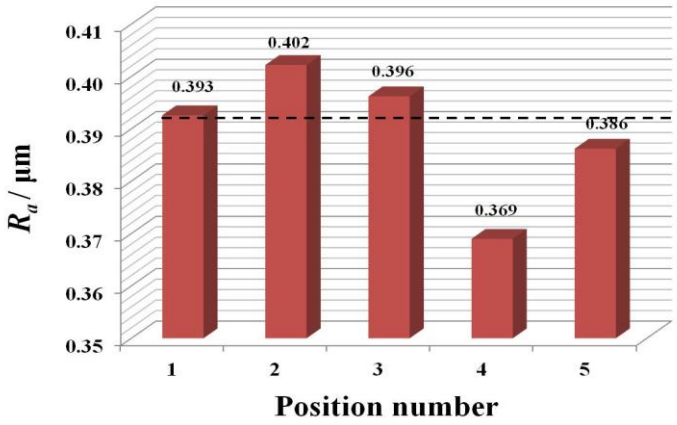

Figure 5.5(a) Mean R_a measurements (from Table 4.4 data) at each of five positions using the VSI. The dashed line is the average value (0.389 µm) calculated from all positions.

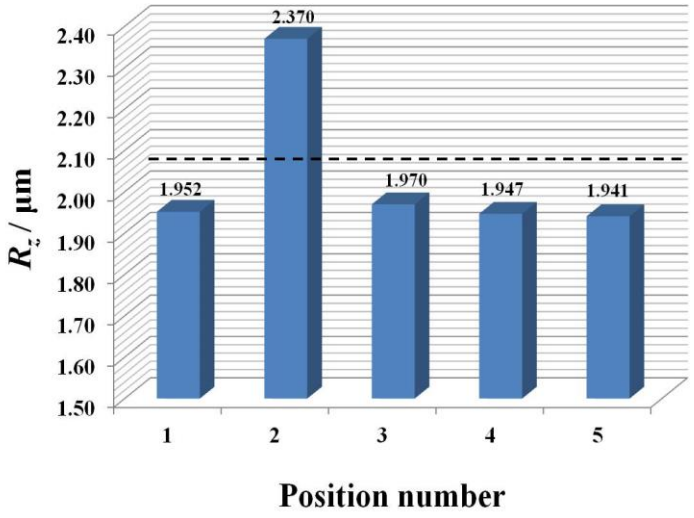

Figure 5.5(b) Mean R_z measurements (from Table 4.4 data) at each of five positions using the VSI. The dashed line is the average value (2.036 µm) calculated from all positions.

Apart from significantly greater standard deviations compared to the stylus method, one other feature is apparent from the data presented in Table 5.4 – a significant systematic scatter between positions that was not observed on the stylus instrument. Standard deviations within the five-measurement groups are significantly smaller than the standard deviation of the data set as a whole which can be clearly seen in the visual representations given in Figure 5.5 (a) and (b). It is clear that the VSI instrument returns statistically different values for different areas within the sample. This may be natural – because the roughness measures refer to maximum and minimum values *across the sample*, in a sufficiently heterogeneous sample there could be significant differences between individual areas.

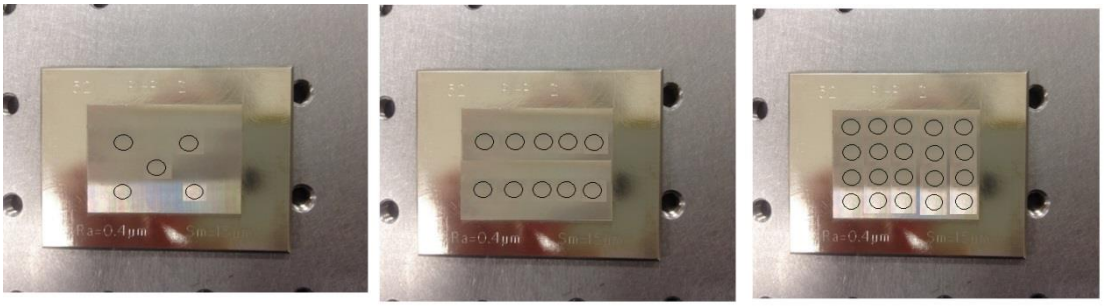

Figure 5.6 The areas of the roughness standard used for the five-position (left), ten-position (middle) and twenty-position (right) VSI measurements reported in this section.

To investigate this matter further, a longer series of measurements was performed on the same sample as shown in Figure 5.6. The measurement results are also presented in Table 5.5 below for both roughness parameters, R_a and R_z.

Table 5.5 Measured roughness values for the standard with Ra = 0.400 µm, Rz = 1.500 µm using the VSI method. A ten-position data set.

Measurement position (scan number)	Arithmetic Mean R_a (µm)	Max. peak to valley R_z (µm)
Position 1		
1	0.461	2.218
2	0.463	2.257
3	0.459	2.187
4	0.462	2.229
5	0.460	2.199
Position 2		
1	0.423	2.411
2	0.422	2.390
3	0.424	2.431
4	0.421	2.370
5	0.420	2.349
Position 3		
1	0.387	1.994
2	0.385	1.935
3	0.386	1.953
4	0.383	1.901
5	0.389	1.982
Position 4		
1	0.409	2.326
2	0.407	2.293
3	0.405	2.257
4	0.406	2.275
5	0.403	2.223
Position 5		
1	0.397	1.870
2	0.392	1.811
3	0.399	1.880
4	0.391	1.899
5	0.400	1.890

Position 6		
1	0.370	2.689
2	0.367	2.649
3	0.362	2.730
4	0.360	2.699
5	0.369	2.680
Position 7		
1	0.466	2.198
2	0.469	2.239
3	0.469	2.218
4	0.472	2.301
5	0.469	2.239
Position 8		
1	0.370	1.988
2	0.366	1.908
3	0.368	1.938
4	0.369	1.949
5	0.367	1.908
Position 9		
1	0.370	1.990
2	0.367	1.931
3	0.365	1.912
4	0.366	1.921
5	0.362	1.901
Position 10		
1	0.442	2.043
2	0.446	2.100
3	0.442	2.049
4	0.446	2.098
5	0.444	2.072
Mean	**0.408**	**2.158**
Standard deviation	0.038	0.248

It has been shown that the R_a measurement of the roughness standard shows the error +0.008 µm with the random error (SD) about 0.038 µm, whilst the R_z measurement shows the error +0.658 µm with the random error (SD) about 0.248 µm. It is clear from the table that the same phenomenon is also present in this longer data series that the results within individual groups show good reproducible, but the inter-group data presents more fluctuation. This inter-group scatter is very apparent in the visual data representation shown in Figure 5.7 below.

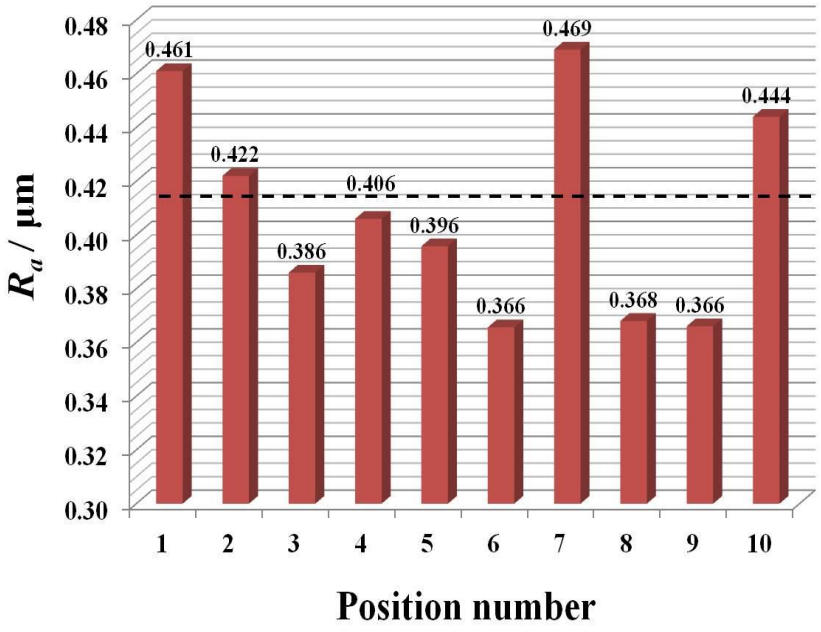

Figure 5.7(a) Mean R_a measurements (from Table 5.5 data) at each of ten positions using the VSI. The dashed line is the average value (0.408 µm) calculated from all positions.

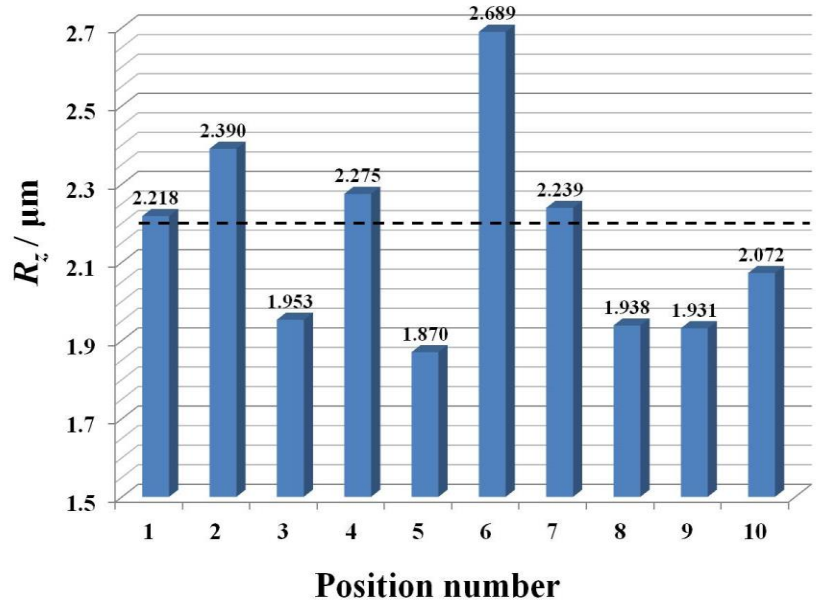

Figure 5.7(b) Mean R_z measurements (from Table 5.5 data) at each of ten positions using the VSI. The dashed line is the average value (2.158 µm) calculated from all positions.

It is now clear that the standard deviation caused by the group scatter is very large compared to the stylus method.

To lay this matter completely to rest, a very long series of measurements was collected, with twenty sample positions used. The data is presented in Table 5.6 below.

Table 5.6 Measured roughness values for the standard with Ra = 0.400 µm, Rz = 1.500 µm using the VSI method. A twenty-position data set.

Measurement position (Scan number)	Arithmetic mean R_a (µm)	Max. peak to valley R_z (µm)
Position 1		
1	0.411	2.113
2	0.409	2.020
3	0.414	2.208
4	0.416	2.233
5	0.405	1.998
Position 2		
1	0.382	1.900
2	0.388	1.939
3	0.385	1.963
4	0.395	1.946
5	0.390	1.956
Position 3		
1	0.384	2.695
2	0.384	2.612
3	0.389	2.751
4	0.380	2.588
5	0.382	2.600
Position 4		
1	0.354	1.918
2	0.354	1.949
3	0.355	1.964
4	0.355	1.962
5	0.358	1.988
Position 5		
1	0.393	1.832
2	0.395	1.889
3	0.393	1.842
4	0.395	1.875
5	0.394	1.867

Position 6		
1	0.474	2.482
2	0.473	2.472
3	0.475	2.492
4	0.472	2.462
5	0.476	2.503
Position 7		
1	0.467	2.329
2	0.468	2.339
3	0.469	2.349
4	0.468	2.339
5	0.468	2.340
Position 8		
1	0.334	1.774
2	0.336	1.794
3	0.333	1.751
4	0.333	1.761
5	0.329	1.703
Position 9		
1	0.382	1.814
2	0.386	1.820
3	0.384	1.818
4	0.384	1.817
5	0.384	1.817
Position 10		
1	0.377	1.987
2	0.375	1.971
3	0.379	2.002
4	0.377	1.988
5	0.377	1.987
Position 11		
1	0.385	1.998
2	0.385	1.986
3	0.384	1.960
4	0.385	2.013
5	0.386	2.020
Position 12		
1	0.326	1.810
2	0.327	1.821
3	0.327	1.821
4	0.328	1.831
5	0.327	1.820

Position 13		
1	0.386	1.998
2	0.385	1.987
3	0.386	1.998
4	0.386	1.997
5	0.387	2.008
Position 14		
1	0.375	2.172
2	0.377	2.273
3	0.373	2.101
4	0.375	2.182
5	0.375	2.183
Position 15		
1	0.371	1.915
2	0.367	1.833
3	0.370	1.894
4	0.368	1.855
5	0.369	1.874
Position 16		
1	0.389	1.779
2	0.387	1.728
3	0.391	1.810
4	0.388	1.759
5	0.390	1.799
Position 17		
1	0.419	2.198
2	0.417	2.188
3	0.417	2.187
4	0.415	2.180
5	0.417	2.189
Position 18		
1	0.382	1.858
2	0.386	1.908
3	0.386	1.908
4	0.389	1.969
5	0.387	1.928
Position 19		
1	0.410	1.970
2	0.412	1.960
3	0.414	1.993
4	0.411	1.951
5	0.409	1.886

Position 20		
1	0.412	1.940
2	0.415	2.024
3	0.413	1.962
4	0.415	1.999
5	0.414	1.981
Mean	**0.391**	**2.029**
Standard deviation	0.035	0.234

It has been shown that the R_a measurement of the roughness standard shows the error -0.009 µm with the random error (SD) about 0.035 µm, whilst the R_z measurement shows the error +0.529 µm with the random error (SD) about 0.234 µm.

The clear conclusion from this table is that it is imperative that a large number of different sample areas are used in VSI measurement because the consequences of using just one position may be catastrophic – the deviations of individual measurement groups seen in Figure 5.8 below can be as high as 20%.

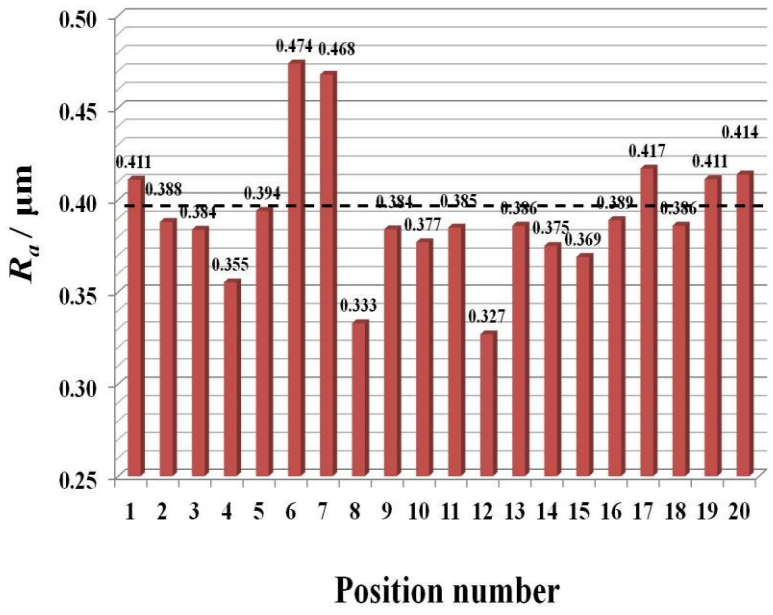

Figure 5.8(a) Mean R_a measurements (from Table 4.6 data) at each of twenty positions using the VSI. The dashed line is the average value (0.391 µm) calculated from all positions.

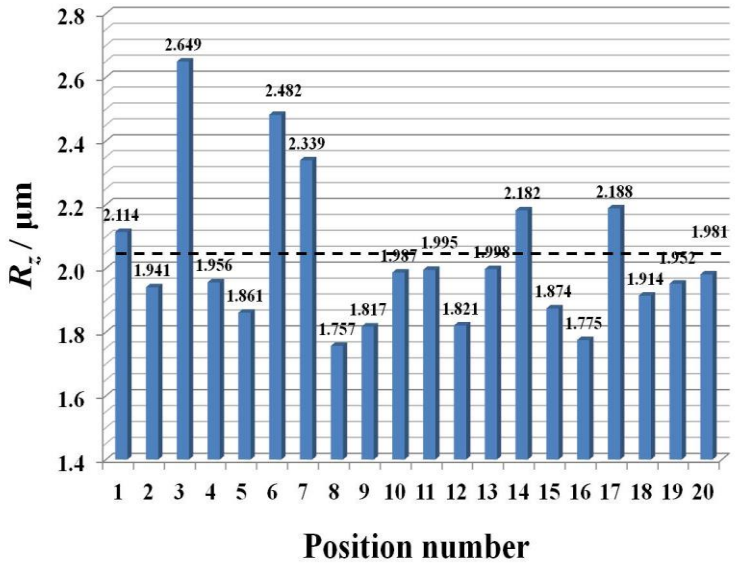

Figure 5.8(b) Mean R_z measurements (from Table 4.6 data) at each of twenty positions using the VSI. The dashed line is the average value (2.029 µm) calculated from all positions.

Such extraordinary lack of reliability for a single-position VSI measurement is quite unexpected for an optical method because the consequences of using just one position may be catastrophic. In future work it would be appropriate to repeat these measurements using a different instrument and standard sample because the data reported above, from general physical principles, are quite hard to accept as valid. In the discussion below we would nonetheless proceed on this assumption.

5.5 Comparison of stylus and VSI methods

Clearly, the values obtained for the step height and roughness standard (R_a and R_z) using contact and non-contact profiling methods indicate significant differences value compared with each other and with the nominal values for the sample. This section contains a discussion of this matter.

5.5.1 Step height measurement

Figure 5.9 shows the mean values (averaged over all five measuring positions taken) for the stylus profilometer and the VSI instrument. The stylus instrument averages of 0.321 and 2.325 microns and VSI instrument averages of 0.366 and 2.414 microns were both in agreement with

the nominal values for the step height (0.330 and 2.340 microns) although the stylus data was clearly more accurate and had a greater repeatability (smaller σ values).

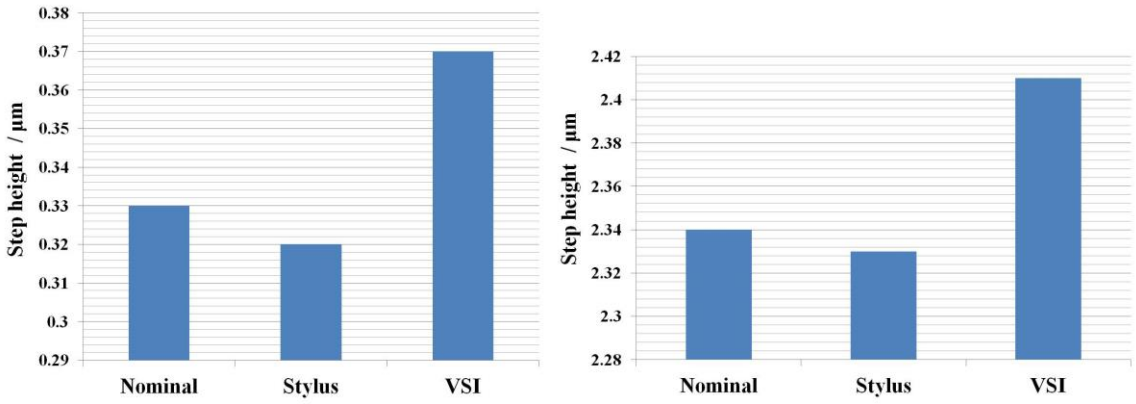

Figure 5.9 Comparison of instrument-derived measured step height values (averaged over all measurement positions) for the quartz glass sample surface.

Looking more closely at the stylus data (Figure 5.1a), two of the data points lay above this average and three points below, with a spread of values from 0.319 µm (min) to 0.324 µm (max), *i.e.* a range of just 5 nm from lowest to highest values. Figure 5.1b shows a range of 13 nm. The VSI data (Figure 5.3) also shows two data points lying above and three below the overall calculated average with values ranging from 0.354 µm to 0.391 µm (Figure 5.3a), *i.e.* a range of 37 nm, whilst in Figure 5.3b the range is 179 nm. The data therefore suggests that for measuring comparatively small step heights (below 1 micron), either technique will give an accurate determination, while the stylus method appears to be the more accurate method for larger step heights.

5.5.2 Average roughness parameter

Figure 5.10 shows the mean values (averaged over all the respective measuring positions taken) for the stylus profilometer and the VSI instrument. The stylus instrument average of 0.385 µm compared impressively well with the nominal 0.400 µm value. Similarly, the VSI data gave excellent agreement with the nominal value with little variation between the values obtained from varying scan numbers (R_a = 0.389 µm (five-position data set), 0.408 µm (ten-position data set) and 0.391 (twenty-position data set)).

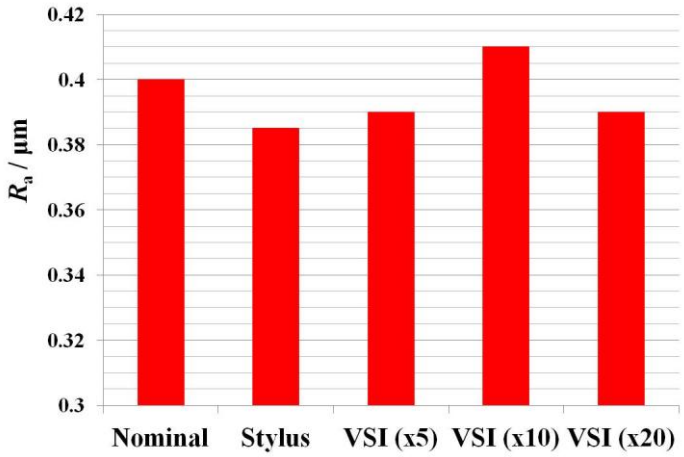

Figure 5.10 Comparison of instrument-derived measured average roughness parameter (R_a) values (averaged over all measurement positions) for the sample surface.

As with the 'small' step height data, the R_a data indicates that both methods are equally valid and accurate for the measurement of the arithmetic mean roughness parameter. In terms of data repeatability, the σ value for the stylus method was significantly lower (0.0035) than for VSI (Figures 5.4, 5.5 and 5.7) for which σ(five-position) = 0.012, σ(ten-position) = 0.038 and σ(twenty-position) = 0.035.

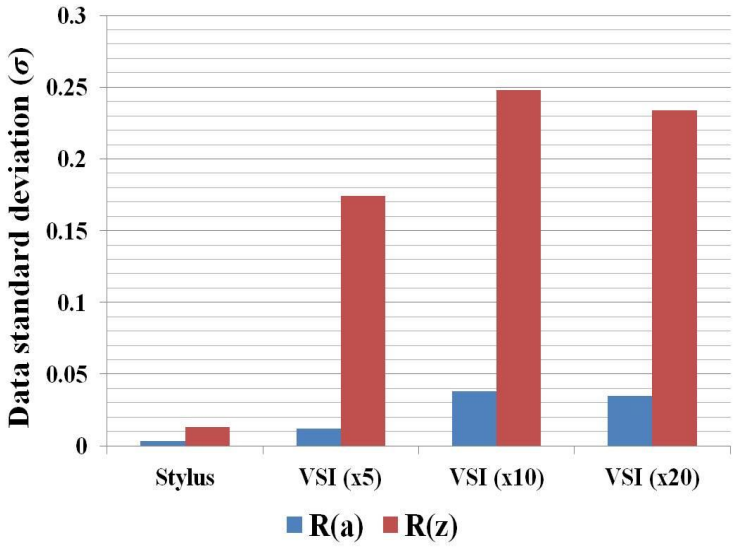

Figure 5.11 Comparison of standard deviation levels for the data sets obtained from stylus and VSI surface profiling.

It is clear that the stylus method is superior in this case as well.

5.5.3 Maximum peak to valley roughness parameter

Figure 5.12 shows the mean values (averaged over all the respective measuring positions taken) for the stylus profilometer and the VSI instrument. The stylus instrument average of 1.449 µm (nominal = 1.500 µm) was significantly more accurate than any of the VSI-derived values that all significantly over-estimated R_z and displayed no improved accuracy as a result of increased scan number (2.036 (x5), 2.158 (x10) and 2.029 (x20)). The standard deviation of the respective data sets implies much greater repeatability as well as accuracy in the case of the stylus method (σ = 0.013) compared with VSI (0.174 (x5), 0.248 (x10) and 0.234 (x20)) – see Figure 5.11.

Generally, the over-estimation and poor repeatability of the VSI data is the influence of unwanted light reflection and diffraction effects during the measurements. Such effects are resolution dependent and therefore with more time available for further data acquisition under other resolution settings, it may have been possible to reduce their influence most and improve the data accuracy and repeatability.

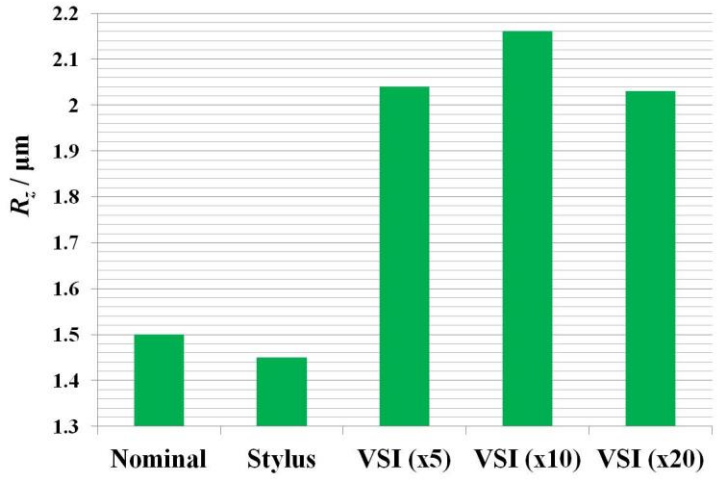

Figure 5.12 Comparison of instrument-derived measured maximum peak to valley roughness parameter (R_z) values (averaged over all measurement positions) for the sample surface.

5.5.4 Previous comparable case studies

A handful of studies have been reported in the literature that describe a similar inter-comparison of different profiling methods and their relative merits with regard to the roughness parameters measured in each case. For example, (Poon and Bhushan, 1995) describe roughness data for a glass-ceramic disc acquired using stylus (two different instruments with

different tip sizes/loadings), optical interferometry and AFM methods. Roughness parameters recorded were the RMS, peak to valley and peak to mean, of that only the one (peak to valley - R_z) was measured in the current study. The R_z data varied greatly in the work of Poon and Bhushan – from 10.0 nm (interferometry) to 23.1 nm**.** The authors concluded that the instrument spatial resolution is a key factor; the lower the resolution, the greater is likely to be the under-estimation in measured parameters. For the three methods that were used in the 1995 study, AFM had the highest resolution, followed by the stylus instrument and lastly the optical method. Where AFM is the most suitable measuring method for surface measurement, it was recommended that the stylus method is preferable but only with a fine tip size (0.2 microns).

A second example is the study of (Rhee et al., 2006) that reported arithmetic mean roughness (R_a) parameter measurements made on a number of standard substrates (etched periodic-spacing diffraction gratings with a variety of nominal R_a values) using a stylus instrument, white light scanning interferometry (WLSI) and phase shifting interferometry (PSI). The study concluded that within certain R_a ranges, the performance of different methods varied significantly and therefore the choice of a single method is strongly dependent on the degree of surface roughness. For R_a of the order of 0.5 microns, the stylus (using a tip of 2 micron radius) and WLSI data was comparable and gave the best agreement with nominal surface values. At lower roughness (50-300 nm), the stylus and WLSI data show greater divergence (due most likely to a 'skewing' effect in the WLSI method) and the PSI data is more consistent with that from the stylus method.

Another recent work (Vorburger et al., 2007) has tested periodic grating standards and roughness standards with Ra values from sub-nanometer to 500 nm. They found that the discrepancy between optical and stylus instruments shows a correlation with Ra. The discrepancy is particularly prominent for Ra between 100 and 200 nm, which is a transition zone between smooth (specular) surfaces and rough (diffuse) surfaces. The discrepancy appeared not to be instrument or sample-dependent. It was also unrelated to the spatial resolution of the instruments used.

A final example is that of (Jouini et al., 2009) who reported R_a values for precision cut aluminum and steel surfaces measured using a stylus method (diamond tip of 2 micron radius / 50 mN load), WLSI and AFM. This study found good agreement in data for the stylus and AFM methods although the stylus instrument is optimal for study of 'macro roughness' surfaces (R_a = 1-10 microns). In contrast the WSLI instrument under-estimated values in the case of aluminum but over-estimated for the steel surfaces as a result of 'smoothing' effects.

In my experiment roughness parameter, Rz measured by White Light interferometry has significant error because the areas of measurement depended on the ability of camera located in the instrument. When the field of view is small, it directly affected the selection of measurement area. For example, if a chosen area has some slight scratches on the surface, it would cause the changes in the Rz value. The Rz value could present higher value than true value. Moreover Rz values also depend on the resolution of an instrument. For Non-contact Measurement high resolution of instrument is recommended. The results from high resolution instrument will demonstrate an appropriate result with less variation, compared with other measurement instrument. These can be compared with the experiment results from Poon and Bhushan (1995). In their experiment Rz value varied from 10 nm to 23.1 nm. When instrument was changed to AFM instrument with high resolution, the error of measurement was decreased.

In addition, the material of the sample also directly affected the measurement of Non-Contact type because of the material property. For example, the difference in absorption, reflection and scattering of the material can influence the measurement error. According to Jouini's experiment (Jouini et al., 2009), when material made of aluminum was measured, the results showed significant lower than (conventional) true value. On the other hand, when metal sample has highly uniform surface, the measurement results presented higher value. These can be implied from the difference in reflection of both materials and it can directly affect the measurement error. Therefore, the selection of measurement instruments suitable for the measured materials is important factor in order to avoid /reduce the measurement error.

Chapter 6

6. Conclusion and Future work recommendations

6.1 Conclusions

The data obtained for step height and roughness standard (R_a and R_z) for the sample surface showed both similarities and key differences between the stylus (contact) and optical (non-contact) measurement methods used in this study.

Firstly, for the smaller step height measurement (nominal value of 0.330 microns), both methods showed high accuracy whilst at the larger step height (2.340 microns), the VSI data was significantly less accurate (and with poorer repeatability – higher data standard deviation) than the stylus method.

Secondly, with regard to the measured roughness parameter data, for the arithmetic mean (R_a) both methods provided excellent accuracy compared with the nominal value (0.4 microns) for the test substrate. Although inherently more variable in nature, the R_z parameter values obtained from the stylus method were in much closer agreement with the nominal value (1.5 microns) than the VSI data that seriously over-estimated (by 35%) across the different scan numbers used (x5, x10 and x20), probably as a result of 'contaminating' optical effects at the resolution settings chosen.

Although the data and conclusions drawn seem reasonably convincing in terms of identifying whether a single technique is sufficient for surface profiling, the study shows the great benefit of a multi-technique approach in identifying the likely strengths and weaknesses of individual methods for individual surfaces and specific parameter determination. It is evident from the findings of the experimental data described in this study that the choice of a single surface profiling technique for the purpose of measuring a number of different parameters is fraught with potential over-estimation of roughness parameters, and therefore very careful consideration must be given to the nature of the surface itself (the scale of roughness – macro vs. micro). It seems clear that, subject to availability, the best option would be a combination of methods using AFM/STM for an accurate assessment of a surface profile in preference to

reliance upon just one method. Each has its inherent positive points that can result in greater measurement accuracy depending upon the surface itself and the choice of parameters being used to describe the surface properties.

6.2 Future work recommendations

Instruments and methods (contact and non-contact) for measuring surface texture have advantages and disadvantages, depending on the precise nature of the material and the specific requirements for data acquisition. From the experiments reported in this thesis, the stylus instrument was generally more accurate (compared with the nominal values for the sample) than the VSI instrument. The VSI instrument (at certain dimensions) showed higher parameter values than those from the stylus instrument. In particular, the R_z value was significantly over-estimated and data repeatability was comparatively poor. Generally, the VSI data over-estimation and poor repeatability is the influence of unwanted light reflection and diffraction effects during the measurements.

Although the stylus instrument returned generally accurate and repeated data, it is important to note that there is the potential for damage to the surface being studied. This damage would depend on the measurement force and the stylus tip size, as well as relative to the hardness of the surface. The white-light interferometry technique would be preferable for measuring profiles of delicate objects or soft materials if the possibility of damage is a concern. Optical methods also have the advantage of higher acquisition speed compared to the stylus instrument, which requires mechanical scanning of the sample area. Optical methods are also sensitive not only to the surface height, but also to slopes and intrinsic optical properties. Fine surface features can cause reflection and diffraction. In deep valleys multiple scattering may occur. Optical method can also produce stray light by scattering from surfaces – all of this can influence the accuracy of the measurement result.

Both vertical scanning interferometry and stylus instrument have become commonplace and the majority of academic and industrial laboratories have both available for use. Where this is the case, and time/costs permit, it necessary to continue to collect data on any future reference surfaces using both methods to identify any significant material-dependent, dimension-dependent and parameter-dependent variation (R_q,$R_{sk,}$ R_{ku} R_v and R_p). The inter-technique

variations reported for the tungsten sample in this thesis may be very different for other types of industrial important surfaces (those having a different material composition), as reported in previous studies published in the literature and reviewed above. For example, the optical effects that were observed for the tungsten surface using VSI may be present to a lesser of degree for single/double element metallic surfaces or for ceramic surfaces of varying roughness dimensions (*i.e.* sub-micron versus super-micron). Future studies of these surface types, at varying roughness, using various multi method approaches would be essential for categorizing any material-specific problems arising from either contact or non-contact characterization methods.

An important consideration for future work is the standardization of samples and instruments used for comparing methods – relative merits and relative performance of different methods tend to depend strongly on non-scientific factors, such as instrument price. Such factors are nonetheless critical in all practical applications and therefore comparisons that are normalized "per unit budget" are potentially more meaningful: it is clear that a sophisticated VSI instrument is more expensive than a simple stylus instrument and a sophisticated stylus instrument is more expensive than a cheap VSI one. It does therefore seem appropriate that future comparisons are performed on a broad (representative of the industrial reality) set of extremely well characterized samples using instruments that cost approximately the same amount. A comparison that does not conform to such criteria runs the risk of being meaningless for all practical purposes – a manager deciding on spending £100k on a new instrument would not find a comparison between a £10k stylus instrument and a £1M VSI instrument in any way useful. Another important factor from the same category is the existence of institutional bias in the evaluation and decision-making process – it is hard to expect that manufacturers of scientific equipment would be prepared to give an equal say to their direct competitors and would not be prepared to exert pressure on those publishing unfavorable reviews. It does therefore seem appropriate that future comparisons are carried out in Academia, which can lay a reasonable claim to impartiality.

As also outlined in this thesis, many other roughness parameter-types can be used to define a surface in addition to the arithmetic mean and maximum peak-valley reported here for the

tungsten sample investigated. For the tungsten surface and for the other types proposed for study above in the future, it may well be the case that inter-method differences occur in reporting different parameters. Future detailed characterization of specific material surfaces (and their inherent roughness variations) would require the measurement and reporting of an additional one or two roughness parameters (*i.e.* R_q – root mean squared altitude deviation) in order to more fully categorize any limitation with individual methods.

Several instruments for measuring surface texture, such as a stylus-based one, or optical/scanning-based methods, such as an atomic force microscopy (AFM), scanning tunneling microscopy (STM), coherence scanning microscope (CSM) and confocal microscopy may be used to compare texture measurements of test specimens. Physical properties of the material under study can also be an important factor in determining the relative accuracy of different instrument types. For the future work, it is suggested that several different materials be used for study to compare the accuracy and repeatability of data acquired by such a range of different methods. In addition, the different stylus sizes should be investigated, as this factor is important in controlling the measurement accuracy for stylus instruments. The stylus tip radius plays an important role in the measurement of surface topography. The surface topography was distorted depending on its stylus tip of finite sizes. In future the mathematical modeling will be investigated for resolving the reconstruction of measured surface topography.

References

ARVINTH DAVINCI, M., PARTHASARATHI, N. L., BORAH, U. & ALBERT, S. K. 2014. Effect of the tracing speed and span on roughness parameters determined by stylus type equipment. *Measurement,* 48**,** 368-377.

ASME-B46.1 2009. Surface Texture (Surface Roughness, Waviness, and Lay).

ATKINS, P. W. & DE PAULA, J. 2010. *Physical chemistry,* New York, W.H. Freeman.

BATCHELOR, A. W., LOH NEE, L. & CHANDRASEKARAN, M. 2011. *Materials degradation and its control by surface engineering*, Imperial College Press.

BHUSHAN, B. 2001. *Modern tribology handbook,* Boca Raton, FL, CRC Press.

BINNIG, G. & ROHRER, H. 1987. Scanning Tunneling Microscopy - from Birth to Adolescence. *Angewandte Chemie-International Edition in English,* 26**,** 606-614.

CLARK, S. R. & GREIVENKAMP, J. E. 2002. Ball tip-stylus tilt correction for a stylus profilometer. *Precision Engineering-Journal of the International Societies for Precision Engineering and Nanotechnology,* 26**,** 405-411.

CONROY, M. & ARMSTRONG, J. 2006. A comparison of surface metrology methods. *Optical Micro- and Nanometrology in Microsystems Technology,* 6188**,** B1880-B1880.

CONROY, M. & MANSFIELD, D. 2008. SCANNING INTERFEROMETRY: Measuring microscale devices. *Nature Photonics,* 2**,** 661-663.

CREATH, K. 1987. Step height measurement using two-wavelength phase-shifting interferometry. *Applied Optics,* 26**,** 2810-2816.

DANZEBRINK, H. U., KOENDERS, L., WILKENING, G., YACOOT, A. & KUNZMANN, H. 2006. Advances in scanning force microscopy for dimensional metrology. *Cirp Annals-Manufacturing Technology,* 55**,** 841-878.

DAVIS, J. R. 2001. *Surface engineering for corrosion and wear resistance,* Materials Park, OH, ASM International : Institute of Materials.

DINIZ, P. S. R., DA SILVA, E. A. B. & NETTO, S. L. 2010. *Digital signal processing : system analysis and design,* New York, Cambridge University Press.

DUBOIS, J.-M. & BELIN-FERRÉ, E. 2011. *Complex metallic alloys : fundamentals and applications,* Weinheim, Wiley-VCH.

EVANS, C. J. & BRYAN, J. B. 1999. "Structured", "textured" or "engineered" surfaces. *Cirp Annals 1999: Manufacturing Technology, Vol 48 No 2 1999***,** 541-556.

GADELMAWLA, E. S., KOURA, M. M., MAKSOUD, T. M. A., ELEWA, I. M. & SOLIMAN, H. H. 2002. Roughness parameters. *Journal of Materials Processing Technology,* 123**,** 133-145.

GAO, F., LEACH, R. K., PETZING, J. & COUPLAND, J. M. 2008. Surface measurement errors using commercial scanning white light interferometers. *Measurement Science & Technology,* 19.

GUO, L., LIU, X. J., ZHOU, L. P., LU, W. L., ZHONG, W. B. & LUO, Y. 2013. A Verification Device for the Stylus Profilometer Sensor. *Sixth International Symposium on Precision Mechanical Measurements,* 8916.

HARIHARAN, P. 2007. B*asic of interferometry,* Amsterdam ; Boston, Elsevier Academic Press.

HARIHARAN, P. 2003. *Optical interferometry,* Amsterdam ; Boston, Academic Press.

HOCKEN, R. J., CHAKRABORTY, N. & BROWN, C. 2005. Optical metrology of surfaces. *Cirp Annals-Manufacturing Technology,* 54**,** 705-719.

ISO4287 1997. Geometrical product specifications. *Terms, definitions and surface texture parameters.*

ISO4288 1996. Geometrical product specifications. *Rules and procedures for the assessment of surface texture.*

ISO5436 2000. Geometrical product specifications. *Measurement standards.*

ISO25178 2012. Geometrical product specifications. *Calibration and measurement standards for geometrical contact (stylus) instruments.*

James C. W. 1995. White Light Interferometry. *Proc. SPIE* 4737, 98-107.

JIANG, X., SCOTT, P. J., WHITEHOUSE, D. J. & BLUNT, L. 2007b. Paradigm shifts in surface metrology. Part II. The current shift. *Proceedings of the Royal Society a-Mathematical Physical and Engineering Sciences,* 463**,** 2071-2099.

JIANG, X. J. & WHITEHOUSE, D. J. 2012. Technological shifts in surface metrology. *Cirp Annals-Manufacturing Technology,* 61**,** 815-836.

JOUINI, N., GAUTIER, A., REVEL, P., MAZERAN, P. E. & BIGERELLE, M. 2009. Multi-scale analysis of high precision surfaces by Stylus Profiler, Scanning White-Light Interferometry and Atomic Force Microscopy. *International Journal of Surface Science and Engineering,* 3**,** 310-327.

JÜTTNER, K. 1990. Electrochemical impedance spectroscopy (EIS) of corrosion processes on inhomogeneous surfaces. *Electrochimica Acta,* 35**,** 1501-1508.

LEACH, R. & HAITJEMA, H. 2010. Bandwidth characteristics and comparisons of surface texture measuring instruments (vol 21, 032001, 2010). *Measurement Science & Technology,* 21.

LEACH, R. K. 2001. *Measurement Good Practice Guide: The Measurement of Surface Texture using Stylus Instruments*, National Physical Laboratory.

LEACH, R. K. 2008. *Measurement Good Practice Guide: Guide for the Measurement of Smooth Surface Topography using Coherence Scanning Interferometry*, National Physical Laboratory.

LEE, D. H. & CHO, N. G. 2012. Assessment of surface profile data acquired by a stylus profilometer. *Measurement Science & Technology,* 23.

LEHMANN, P., KUHNHOLD, P. & XIE, W. C. 2014. Reduction of chromatic aberration influences in vertical scanning white-light interferometry. *Measurement Science & Technology,* 25.

LEIS, J. 2011. *Digital signal processing using MATLAB for students and researchers,* Hoboken, New Jersey, Wiley.

LONARDO, P. M., LUCCA, D. A. & DE CHIFFRE, L. 2002. Emerging trends in surface metrology. *Cirp Annals-Manufacturing Technology,* 51**,** 701-723.

MATHIA, T. G., PAWLUS, P. & WIECZOROWSKI, M. 2011. Recent trends in surface metrology. *Wear,* 271**,** 494-508.

MCCOOL, J. I. 1984. Assessing the Effect of Stylus Tip Radius and Flight on Surface-Topography Measurements. *Journal of Tribology-Transactions of the Asme,* 106**,** 202-210.

MICHELSON, A. A. & MORLEY, E. W. 1887. On the relative motion of the Earth and the luminiferous ether. *American Journal of Science,* Series 3 Vol. 34**,** 333-345.

MORRISON, E. 1995. A Prototype Scanning Stylus Profilometer for Rapid Measurement of Small Surface-Areas. *International Journal of Machine Tools & Manufacture,* 35**,** 325-331.

NIEHUES, J., LEHMANN, P. & BOBEY, K. 2007. Dual-wavelength vertical scanning low-coherence interferometric microscope. *Applied Optics,* 46**,** 7141-7148.

PAWLUS, P. & SMIESZEK, M. 2005. The influence of stylus flight on change of surface topography parameters. *Precision Engineering-Journal of the International Societies for Precision Engineering and Nanotechnology,* 29**,** 272-280.

POON, C. Y. & BHUSHAN, B. 1995. Comparison of surface roughness measurements by stylus profiler, AFM and non-contact optical profiler. *Wear,* 190**,** 76-88.

RAJA, J., MURALIKRISHNAN, B. & FU, S. 2002. Recent advances in separation of roughness, waviness and form. *Precision Engineering-Journal of the International Societies for Precision Engineering and Nanotechnology,* 26**,** 222-235.

RHEE, H.-G., LEE, Y.-W., LEE, I.-W. & VORBURGER, T. V. 2006. Roughness Measurement Performance Obtained with Optical Interferometry and Stylus Method. *Journal of the Optical Society of Korea,* 10**,** 48-54.

RHEE, H. G., VORBURGER, T. V., LEE, J. W. & FU, J. 2005. Discrepancies between roughness measurements obtained with phase-shifting and white-light interferometry. *Applied Optics,* 44**,** 5919-5927.

SHERRINGTON, I. & SMITH, E. H. 1988a. Modern Measurement Methods in Surface Metrology .1. Stylus Instruments, Electron-Microscopy and Non-Optical Comparators. *Wear,* 125**,** 271-288.

SHERRINGTON, I. & SMITH, E. H. 1988b. Modern Measurement Methods in Surface Metrology .2. Optical-Instruments. *Wear,* 125**,** 289-308.

SMITH, G. T. 2002. *Industrial metrology : surfaces and roundness,* London ; New York, Springer.

SONG, J. F. & VORBURGER, T. V. 1991. Stylus Profiling at High-Resolution and Low Force. *Applied Optics,* 30**,** 42-50.

TAKADOUM, J. 2008. *Materials and surface engineering in tribology*, Wiley.

TAN, Y. 2013. *Heterogeneous electrode processes and localized corrosion*.

THWAITE, E. G. 1984. Measurement and Control of Surface Finish in Manufacture. *Precision Engineering-Journal of the American Society for Precision Engineering,* 6**,** 207-217.

TODRES, Z. V. 2006. *Organic mechanochemistry and its practical applications,* Boca Raton, FL, CRC/Taylor & Francis.

VORBURGER, T. V., RHEE, H. G., RENEGAR, T. B., SONG, J. F. & ZHENG, A. 2007. Comparison of optical and stylus methods for measurement of surface texture. *International Journal of Advanced Manufacturing Technology,* 33**,** 110-118..

WATTS, R.A.,SAMBLE,J.R., HUTLY,M.C.,PREIST,T.W.&LAWREMCE,C.R.1997. A new optical technique for characterizing reference artefacts for surface profilometry. Ed. Nanotechnology, 8.

WHITEHOUSE, D. J. 1994. *Handbook of surface metrology,* Bristol ; Philadelphia, Institute of Physics Pub.

WHITEHOUSE, D. J. 1997. Surface metrology. *Measurement Science & Technology,* 8**,** 955-972.

WHITEHOUSE, D. J. 2000. Surface characterization and roughness measurement in engineering. *Photo-Mechanics,* 77**,** 413-461.

WHITEHOUSE, D. J. 2011. *Handbook of surface and nanometrology,* Boca Raton, CRC Press.

ZHOU, Y. & BREYEN, M. D. 2010. *Joining and assembly of medical materials and devices*.